JOURNAL OF VIROLOGY, Oct. 2011, p. 10582–10597 Vol. 85, No. 20
0022-538X/11/$12.00 doi:10.1128/JVI.00671-11

Anti-Severe Acute Respiratory Syndrome Coronavirus Spike Antibodies Trigger Infection of Human Immune Cells via a pH- and Cysteine Protease-Independent FcγR Pathway▽

Martial Jaume,[1]* Ming S. Yip,[1] Chung Y. Cheung,[2] Hiu L. Leung,[1] Ping H. Li,[1] Francois Kien,[1] Isabelle Dutry,[1,2] Benoît Callendret,[3,4]‡ Nicolas Escriou,[3,4] Ralf Altmeyer,[1]† Beatrice Nal,[1,5] Marc Daëron,[6,7] Roberto Bruzzone,[1,8] and J. S. Malik Peiris[1,2]

HKU-Pasteur Research Centre, 8 Sassoon Road, Hong Kong SAR, People's Republic of China[1]; Department of Microbiology, The University of Hong Kong, 21 Sassoon Road, Hong Kong SAR, People's Republic of China[2]; Institut Pasteur, Unité de Génétique Moléculaire des Virus à ARN, Département de Virologie, 25 Rue du Docteur Roux, F-75015 Paris, France[3]; CNRS, URA30I5, F-75015 Paris, France[4]; Department of Anatomy, The University of Hong Kong, 21 Sassoon Road, Hong Kong SAR, People's Republic of China[5]; Institut Pasteur, Département d'Immunologie, Unité d'Allergologie Moléculaire et Cellulaire, 25 Rue du Docteur Roux, F-75015 Paris, France[6]; INSERM, Unité 760, 25 Rue du Docteur Roux, F-75015 Paris, France[7]; and Institut Pasteur, Department of Cell Biology and Infection, 25 Rue du Docteur Roux, F-75015 Paris, France[8]

Received 4 April 2011/Accepted 5 July 2011

Public health measures successfully contained outbreaks of the severe acute respiratory syndrome coronavirus (SARS-CoV) infection. However, the precursor of the SARS-CoV remains in its natural bat reservoir, and reemergence of a human-adapted SARS-like coronavirus remains a plausible public health concern. Vaccination is a major strategy for containing resurgence of SARS in humans, and a number of vaccine candidates have been tested in experimental animal models. We previously reported that antibody elicited by a SARS-CoV vaccine candidate based on recombinant full-length Spike-protein trimers potentiated infection of human B cell lines despite eliciting *in vivo* a neutralizing and protective immune response in rodents. These observations prompted us to investigate the mechanisms underlying antibody-dependent enhancement (ADE) of SARS-CoV infection *in vitro*. We demonstrate here that anti-Spike immune serum, while inhibiting viral entry in a permissive cell line, potentiated infection of immune cells by SARS-CoV Spike-pseudotyped lentiviral particles, as well as replication-competent SARS coronavirus. Antibody-mediated infection was dependent on Fcγ receptor II but did not use the endosomal/lysosomal pathway utilized by angiotensin I converting enzyme 2 (ACE2), the accepted receptor for SARS-CoV. This suggests that ADE of SARS-CoV utilizes a novel cell entry mechanism into immune cells. Different SARS vaccine candidates elicit sera that differ in their capacity to induce ADE in immune cells despite their comparable potency to neutralize infection in ACE2-bearing cells. Our results suggest a novel mechanism by which SARS-CoV can enter target cells and illustrate the potential pitfalls associated with immunization against it. These findings should prompt further investigations into SARS pathogenesis.

Although public health measures have successfully contained human outbreaks of the severe acute respiratory syndrome coronavirus (SARS-CoV) infection, a disease with a case-fatality ratio of 10% (13, 32), the precursor SARS-CoV-like virus remains endemic in its natural bat reservoir (34), and future reemergence of a SARS-like disease remains a credible public health threat. Therefore, efforts have continued to develop safe vaccine strategies against SARS-CoV.

Neutralizing antibodies are elicited in patients recovering from SARS and studies on experimental animal models have shown that antibodies can prevent infection by SARS-CoV (6). Among the four major structural SARS-CoV proteins, the Spike envelope glycoprotein (S) has been identified as the most important antigen inducing neutralizing and protective antibodies (1, 3, 72). Furthermore, it has been demonstrated that binding of Spike to its receptor angiotensin I converting enzyme 2 (ACE2) is a key event in the entry of SARS-CoV into cells (40).

Several vaccine strategies aiming at preventing infection by SARS-CoV have therefore targeted the Spike glycoprotein (14, 15). Such a strategy, however, poses concern since previous attempts at vaccination against coronaviruses have resulted in markedly different outcomes. Immune protection against animal coronaviruses, such as mouse hepatitis and transmissible gastroenteritis viruses (11, 46), can be induced by immunization with Spike glycoprotein. On the other hand, this vaccine approach led to a worsened disease in the feline coronavirus (FCoV) infection due to the induction of infection-enhancing antibodies (8, 25, 44, 65). Immune-mediated infections and, in particular, antibody-dependent enhancement

* Corresponding author. Mailing address: HKU-Pasteur Research Centre, Dexter H. C. Man Building, 8 Sassoon Road, Pokfulam, Hong Kong SAR, China. Phone: (852) 2816 8423. Fax: (852) 2872 5782. E-mail: breizh@hku.hk.

‡ Present address: Center for Vaccines and Immunity, the Research Institute at Nationwide Children's Hospital, 700 Childrens Dr., Columbus, OH 43205.

† Present address: Institut Pasteur of Shanghai, Chinese Academy of Sciences, Shanghai, People's Republic of China.

▽ Published ahead of print on 20 July 2011.

(ADE) have long been known to be exploited by a variety of viruses, such as dengue virus, HIV, and FCoV, as an alternative way to infect host cells (59, 60). In addition to interaction between viral protein and host receptors, these viruses can enter into cells through binding of virus/antibody immune complexes to Fc receptors (FcR) or complement receptors or, alternatively, by inducing a conformational change in envelope glycoproteins that are required for virus-cell membrane fusion (59, 60). Thus, immunization of cats with recombinant vaccinia virus preparations expressing the FCoV Spike protein resulted in the induction of Spike-specific antibodies responsible for an enhanced susceptibility to challenge infection (65). The enhanced infection of macrophages following antibody-mediated entry of the FCoV is responsible for the occurrence of the severe disease feline infectious peritonitis (8, 25, 44).

We previously reported that a SARS-CoV vaccine candidate based on recombinant, full-length SARS-CoV Spike-protein trimers triggered infection of human B cell lines despite eliciting *in vivo* a neutralizing and protective immune response in rodents (30). These observations prompted us to further investigate the molecular and cellular mechanisms underlying ADE of SARS-CoV infection *in vitro*.

By monitoring the susceptibility of immune cell lines having different patterns of Fcγ receptor (FcγR) expression, we have demonstrated the predominant role of human FcγRII (CD32) in mediating ADE of SARS-CoV. Furthermore, we have provided evidence that, in contrast to the ACE2-mediated infection, ADE pathways are independent of endosomal or lysosomal pH and are minimally affected by the activities of cysteine proteases. Finally, we have found marked differences between different SARS vaccines in their capacity to elicit a humoral immune response that neutralizes or facilitates infection by SARS-CoV *in vitro*, an observation that should prompt further studies to develop safe immunization protocols.

MATERIALS AND METHODS

Cell lines. The following cell lines were used in the present study: VeroE6 (African green monkey kidney epithelial cells), K-562 (human chronic myelogenous leukemia cells), U-937 (human histiocytic lymphoma cells), THP-1 (human acute monocytic leukemia cells), SUP-T1 (human lymphoblastic leukemia/T lymphoblast), MOLT-3 (human acute lymphoblastic leukemia/T lymphoblast), MT4/R5 (human T cell lymphoblast expressing CCR5), Raji (Burkitt's lymphoma/B lymphoblast), Daudi (Burkitt's lymphoma/B lymphoblast), parental ST486 (Burkitt's lymphoma/B lymphoblast lacking expression of FcγR) and FcγR/ST486, 721.221 (Epstein-Barr virus-transfected human B cells), and P388D1 and J774A.1 (murine macrophage-like lymphoblasts). VeroE6 cells were cultured in Dulbecco modified Eagle medium (DMEM) supplemented with 10% of heat-inactivated fetal bovine serum (FBS), and hematopoietic cells were cultured in RPMI 1640 medium supplemented with 10% heat-inactivated FBS, 1% nonessential amino acids, 4 mM L-glutamine, 1 mM sodium pyruvate, and 20 μM β_2-mercaptoethanol (all from Invitrogen). All cells were maintained in a humidified atmosphere at 37°C with a 5% CO_2 supply.

Immunization with recombinant Spike proteins or inactivated SARS-CoV. Recombinant SARS-CoV Spike proteins were produced as described elsewhere (4, 30). Six to eight-week-old BALB/c mice ($n = 4$ to 5 per group) were immunized intraperitoneally with one of the following antigens: 2 μg of recombinant codon-optimized SARS-CoV Spike full-length (S, amino acids [aa] 1 to 1255), 2 μg of recombinant codon-optimized SARS-CoV Spike ectodomain (S.ECD, aa 1 to 1184), 2 μg of recombinant codon-optimized SARS-CoV Spike subunit 1 (S1, aa 1 to 757), or 10 μg of recombinant, soluble SARS-CoV Spike truncated early after the transmembrane domain (Ssol, aa 1 to 1193) (see Fig. 8A for details). All recombinant proteins were FLAG tagged according to standard molecular biology techniques. An additional group, immunized with 2 μg (Spike-equivalent) of gamma-irradiated SARS-CoV virion (^{60}Co based, 50 KGy; whole killed virus [WKV]), was also included, as well as a control group injected with saline solution. Mice received two immunizations in the presence of 1 mg of Alum at 3-week intervals, and blood samples were collected by bleeding the saphenous vein on days −1, 27, and 55 postimmunization in accordance with local guidelines for animal handling. For all groups ($n = 4$ to 5), serum samples were collected at day 55 postimmunization, and an equal volume from each animal was pooled, heat inactivated for 30 min at 56°C, and stored at −20°C for subsequent use.

Production and use of lentiviral pseudotyped particles. The pseudotyped viral particles expressing a luciferase reporter gene were essentially produced as described elsewhere (42). Briefly, SARS-CoV Spike-pseudotyped lentiviral particles (SARS-CoVpp), vesicular stomatitis virus glycoprotein (VSV-G)-pseudotyped lentiviral particles (VSVpp), or lentiviral particles lacking expression of any viral envelope protein (Δenv.pp) were obtained by transfection of HEK293T cells with an HIV-1 provirus construction (pNL4.3.LucR$^-$E$^-$pro$^-$) and a plasmid encoding the viral envelope protein of interest, i.e., SARS-CoV Spike, VSV-G, or empty vector (pcDNA3.1; Invitrogen), respectively. After a purification step on a 20% sucrose cushion, the concentrated viral particles were titrated by enzyme-linked immunosorbent assay (ELISA) for lentivirus-associated HIV-1 p24 protein according to the manufacturer's instruction (Cell Biolabs, Inc.), and the viral stocks were stored at −80°C until use.

For neutralization and ADE assays, 100 μl of serial, 2-fold dilutions of heat-inactivated mouse serum were incubated for 1 h at 37°C with 100 μl of pseudotyped viral particles. The same inoculum was then used to infect in parallel both VeroE6 (SARS-CoVpp neutralization test) and hematopoietic (ADE assay) cells. Briefly, 10^4 VeroE6 cells were seeded 24 h before the infection in a 96-well Opti-plate (Perkin-Elmer). On the day of infection, the cells were washed twice, and 25 μl of inoculum was added to an equivalent volume of supplemented DMEM. Hematopoietic cells were washed and diluted to 2×10^6 cells/ml in supplemented RPMI 1640 medium. Portions (25 μl) of inoculum were deposited in a 96-well Opti-plate, and an equal volume of the cell suspension was added immediately thereafter. After 1 h of incubation at 37°C, the cells were washed and incubated for additional 65 to 75 h in 100 μl of supplemented culture medium. The cells were quenched by adding 100 μl of BrightGlow luciferase substrate (Promega) directly to each well, and the luciferase activity was measured with a MicroBeta Jet counter (Perkin-Elmer). Background values, monitored from uninfected cells and cells infected with lentiviral particles lacking expression of any viral envelope protein (Δenv.pp) were consistently below 200 relative luminescence units (see Fig. 1 for reference).

Infection with SARS-CoV. Serial, 2-fold dilutions of heat-inactivated mouse sera were incubated for 1 h at 37°C with an equal volume of live SARS-CoV (strain HKU-39849) under appropriate containment in a BSL3 laboratory (Department of Microbiology, The University of Hong Kong). Both VeroE6 and Raji cells were infected at a multiplicity of infection (MOI) of 1 for 60 min at 37°C, washed, and then incubated in supplemented culture medium containing appropriate dilutions of mouse serum. At the end of the experiment, the cells were either fixed in 4% paraformaldehyde (dissolved in phosphate-buffered saline) for immunofluorescence microscopy or resuspended in lysis buffer (RLT buffer, RNeasy RNA minikit; Qiagen) for endpoint and real-time quantitative PCR and stored appropriately until use. In addition, samples of the cell culture supernatants (100 μl) harvested at different time points were mixed with 350 μl of RLT buffer and stored at −80°C until use.

Immunofluorescence microscopy. To assess SARS-CoV infection, both VeroE6 and Raji cells were incubated for 45 min with either a mouse monoclonal antibody specific for the viral nucleoprotein (N) (7) or rabbit polyclonal antibodies recognizing the viral membrane (M) protein (ProSci), which were revealed by secondary TRITC (tetramethyl rhodamine isothiocyanate)-conjugated goat anti-mouse (Zymed Laboratories) and fluorescein isothiocyanate (FITC)-conjugated goat anti-rabbit antibody (Jackson Immunoresearch), respectively. Slides were assembled with DAPI (4′,6′-diamidino-2-phenylindole)-containing mounting reagent (Southern Biotech) and analyzed with an AxioObserver Z1 microscope (Zeiss). Pictures from 10 to 30 randomly selected fields were acquired with an Axiocam MRm camera and processed with MetaMorph software (Molecular Devices).

Endpoint and real-time quantitative reverse transcriptase PCR (RT-PCR) for viral gene expression. Total RNAs were extracted with an RNeasy RNA minikit (Qiagen), with DNase digestion, according to the manufacturer's instructions. Extracted RNAs were stored at −80°C until use. Superscript III reverse transcriptase (Invitrogen) and random hexamer primers (Invitrogen) or gene-specific oligonucleotides were used to convert RNAs to cDNAs. The amounts of viral and host RNA were measured either by conventional endpoint PCR or by real-time quantitative PCR using TaqMan MGB probe-based technology on a LightCycler 480-II instrument (Roche). The primers and conditions for detection

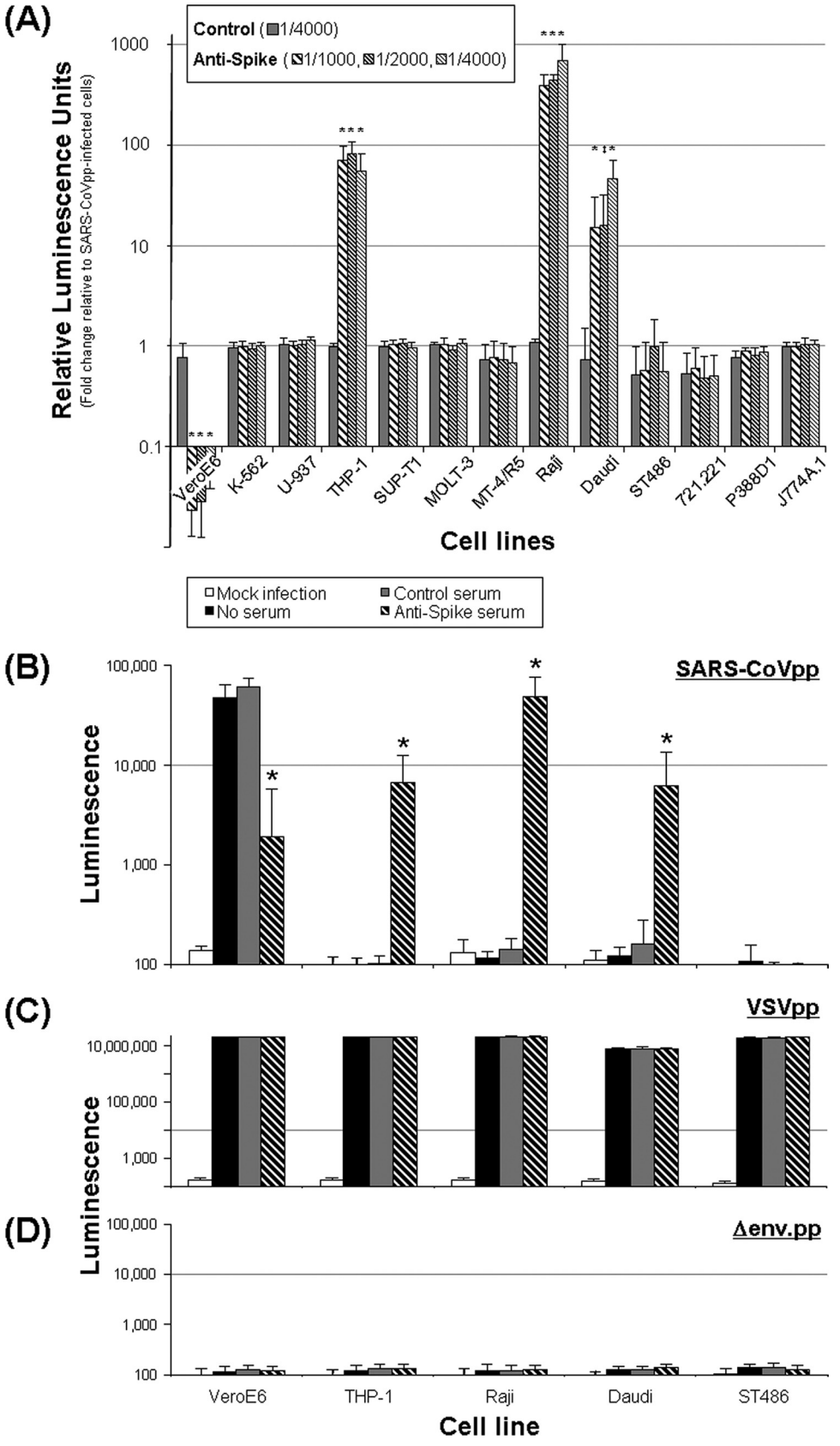
(A)
Control (1/4000)
Anti-Spike (1/1000, 1/2000, 1/4000)
Relative Luminescence Units
(Fold change relative to SARS-CoVpp-infected cells)
1000
100
10
1
0.1
***
VeroE6
K-562
U-937
THP-1
SUP-T1
MOLT-3
MT-4/R5
Raji
Daudi
ST486
721.221
P388D1
J774A.1
Cell lines
Mock infection
No serum
Control serum
Anti-Spike serum
(B)
SARS-CoVpp
Luminescence
100,000
10,000
1,000
100
(C)
VSVpp
10,000,000
100,000
1,000
(D)
Δenv.pp
VeroE6
THP-1
Raji
Daudi
ST486
Cell line

of the GAPDH and SARS-CoV genomic and subgenomic species (18), as well as the SARS-CoV ORF1b and nucleoprotein genes (7), have been described previously. Positive and negative controls were included in each run and, when appropriate, the levels of SARS-CoV gene expression were normalized to those of the 18S rRNA gene, which were determined using 600 nM concentrations of both forward (5′-CggAggTTCgAAgACgATCA-3′) and reverse (5′-ggCgggTCA TgggAATAAC-3′) primers and a 100 nM concentration of the probe (5′HEX-ATACCgTCgTAgTTCCgACCA-BHQ3′).

Human Fcγ receptor profiling by conventional endpoint PCR. Total RNAs were extracted with an RNeasy RNA minikit (Qiagen), with DNase digestion, according to the manufacturer's instructions, and stored at −80°C until use. Superscript III reverse transcriptase (Invitrogen) and random hexamer primers (Invitrogen) were used to convert RNAs to cDNAs. Additional samples consisting of negative RT controls (RT−) were prepared by omitting Superscript III during reverse transcription. The amounts of RNA/cDNA encoding FcεR1γ chain, FcγRIA (CD64a), FcγRIIA (CD32a), FcγRIIB (CD32b), FcγRIIIA (CD16a), ACE2, and GAPDH were measured by conventional endpoint PCR using the primer pairs described in Table 2. Negative and positive controls (i.e., DNA plasmid containing the full coding sequence of the gene of interest) were included in each run. The amplification procedure consisted of an initial denaturation step at 94°C for 5 min, followed by 30 cycles of three steps of 45 s each, including denaturation at 94°C, primer annealing at 60°C, and primer extension at 72°C. The protocol also included a final extension step at 72°C for 7 min. Amplicons were eventually visualized by ethidium bromide staining after electrophoresis in 2% agarose gel, and negative images were taken.

Flow cytometry. Cells were harvested at 4°C in phosphate-buffered saline containing 1% FBS, 2% normal human serum, 3% normal goat serum, 2 mM EDTA, and 0.1% sodium azide and then incubated for 30 to 45 min at 4°C with 1 μg of either isotype-matched control or monoclonal antibody/ml for the indicated human FcγR. The following mouse monoclonal antibodies were used: 3G8 anti-hCD16, 3D3, FLI8.26 anti-hCD32, or 10.1 anti-hCD64 (all from BD Pharmingen) and MOPC-21 (IgG1, κ) or MPC-11 (IgG2b, κ) isotype controls (both from BioLegend). The cells were then washed, and the primary antibody binding was revealed by staining at 4°C for 30 min with FITC-conjugated goat anti-mouse antibodies (Jackson Immunoresearch). Finally, washed cells were further incubated with an optimal concentration of the fixable viability dye eFluor 660 (FVD660; eBioscience). The data were collected from ≥30,000 singlet living cells on a LSRII flow cytometer (BD Biosciences), and postacquisition analyses were performed using the FlowJo software (TreeStar).

Blockade of human Fcγ receptor *in vitro*. Cells were washed with cold, supplemented RPMI 1640 medium and maintained on ice throughout the anti-FcγR blocking step only. Briefly, 2×10^5 cells were treated for 45 to 60 min in 200 μl of supplemented culture medium containing 5 μg of either FcγR-specific mouse monoclonal antibody (3G8, anti-hCD16; FLI8.26, anti-hCD32; and 10.1, anti-hCD64 [BD Pharmingen]) or isotype-matched controls (clone MOPC-21 and MPC-11 [BioLegend])/ml. An equal volume of inoculum was directly added to the tubes, and the samples were incubated at 37°C for 60 min. Cells were washed twice and resuspended in supplemented culture medium (5×10^5 cells/ml), and 100 μl (triplicate) was transferred to a 96-well Opti-plate (Perkin-Elmer). The plates were then incubated at 37°C for 65 to 75 h, and the luciferase activity was measured as described above.

Lentiviral transfer vector construction. We constructed the lentiviral plasmids encoding human FcεRγ-chain and/or human FcγR by substituting enhanced green fluorescent protein (eGFP) and/or hygromycin resistance gene from the bicistronic vector pCHMWS-eGFP_IRES_hygromycin (kindly provided by Rik Gijsbers and Zeger Debyser [Katholieke Universiteit Leuven, Leuven, Belgium]). The FcεRγ-chain coding sequence (GenBank accession no. M33195) was obtained by PCR amplification from the huFcRγ/pBJ1 neo plasmid (kindly provided by Jean-Pierre Kinet [Harvard Medical School, Boston, MA]) (38). The unique restriction sites BamHI and XhoI were added to the 5′ and 3′ ends, respectively. After amplification, the human FcεRγ-chain PCR product was digested with BamHI and XhoI and inserted into the transfer plasmid to yield pCHMWS-huFcεRγ-chain_IRES_hygromycin. The latter construction was used to generate pCHMWS-huFcεRγ-chain_IRES_huFcγRIA and pCHMWS-huFcεRγ-chain_IRES_huFcγRIIIA.

The human FcγRIA (hCD64a) coding sequence (GenBank accession no. NM_000566) was obtained by PCR amplification from the huFcγRIA/pcDNA-1 plasmid (kindly provided by Clark L. Anderson, Ohio State University, Columbus, OH) (41), with BamHI and SpeI linkers at the 5′ and 3′ ends, respectively. After amplification, the human FcγRIA PCR product (1,151 bp) was digested with BamHI and SpeI and inserted into the transfer plasmid digested by BclI and SpeI to yield pCHMWS-huFcεRγ-chain_IRES_huFcγRIA. A human FcγRIIIA (hCD16a) fragment (1,417 bp) was removed from the LL649 plasmid (kindly provided by Lewis L. Lanier, University of California, San Francisco, CA) (33) using BamHI and EcoRI and inserted into the pIRES plasmid (Clontech) using the same restriction enzymes. A cDNA fragment (183 bp) was PCR amplified from human peripheral blood mononuclear cells using the forward (5′-TgACgg ATCCAggAAATTggTgggTgACAg-3′) and reverse (5′-gTCAggATCCTAgCAg AgCAgTTgggAggA-3′) primers, both flanked by an BamHI site, and then inserted into LL649/pIRES plasmid at the BamHI site. The full human FcγRIIIA coding sequence (GenBank accession no. NM_000569) was generated by excision of the undesirable fragment (225 bp) with EcoRV and direct religation, yielding the huFcγRIIIA/pIRES shuttle vector. The human FcγRIIIA fragment was subsequently excised using BamHI and NcoI+Klenow blunting and cloned into the lentiviral vector resulting in pCHMWS-huFcεRγ-chain_IRES_huFcγRIIIA. Coding sequences for human FcγRIIA (hCD32a) isoforms (huFcγRIIA.R131 and huFcγRIIA.H131 GenBank accession no. NM_021642) and human FcγRIIB1 (hCD32b; GenBank accession no. AF543826) flanked by BglII and SalI sites were commercially synthesized (GeneArt, Regensburg, Germany). The synthetic sequences were digested by BglII and SalI and inserted into the original transfer plasmid to yield pCHMWS-huFcγRIIA.R131_IRES_hygromycin, pCHMWS-huFcγRIIA.H131_IRES_hygromycin, and pCHMWS-huFcγRIIB1_IRES_hygromycin. To verify that PCR amplification and cloning procedures had not introduced random mutations, all constructs were sequenced by the Genome Research Centre (The University of Hong Kong).

Generation of FcγR-expressing cell lines using lentiviral particle-based gene transduction. Pseudotyped viral particles were essentially produced as described elsewhere (42). Briefly, VSV-G-pseudotyped lentiviral particles were obtained by transfecting HEK293T cells with a packaging plasmid (pCMVΔR8.91), a plasmid encoding the envelope of VSV (pCI-VSVg), and a pCHMWS-derived transfer plasmid (described above) coding for a human Fc receptor as specified. Stable cell lines were generated by the transduction of monoclonal ST486 cells with the VSV-G-pseudotyped lentiviral particles. Briefly, target cells were washed and diluted to 3×10^6 cells/ml in supplemented RPMI 1640 medium. One milliliter of crude supernatant from pseudoparticle-producing 293T cells was deposited in a 24-well plate, and an equal volume of the cell suspension was added immediately thereafter. After 3 to 8 h of incubation at 37°C, the cells were washed and incubated for additional 40 to 48 h in 2 ml of supplemented culture medium. At 2 days postinfection, the cell surface expression of the human FcγR was monitored by flow cytometry, and the cells were subsequently cultured in selective medium containing 250 μg of hygromycin (Invitrogen)/ml when appropriate. Finally, several monoclonal cell lines for each construct were isolated by Pois-

FIG. 1. Susceptibility of hematopoietic cell lines to infection by SARS-CoV Spike pseudoparticles (SARS-CoVpp). (A) SARS-CoVpp were incubated in the presence or absence of different dilutions (1/1,000, 1/2,000, and 1/4,000) of either control (solid bars) or anti-Spike (hatched bars) serum for 1 h prior to addition to the cells. At 3 days postinfection, luciferase substrate reagent was added to wells, and the luminescence was measured. The data were normalized to control conditions, *viz.*, cells incubated with SARS-CoVpp in the absence of any serum (taken as unity), and are expressed as the fold changes in luminescence. Because the results for SARS-CoVpp with or without control serum were virtually identical with all cell lines, for the sake of clarity only one dilution (1/4,000) is shown. The results are the means ± the SD of six measurements from two independent experiments. Statistical significance was assessed by comparing the appropriate dilutions of control and anti-Spike serum (‡, $P < 0.05$; ⁎, $P < 0.001$ [unpaired Student *t* test]). (B to D) HIV Gag-normalized lentiviral particles (0.1 ng of p24 protein/μl) pseudotyped with the envelope glycoprotein of SARS-CoV Spike (SARS-CoVpp [B]) or vesicular stomatitis virus (VSVpp [C]) or lacking any viral envelope protein (Δenv.pp [D]) were incubated in the presence or absence of a 1/1,000 dilution of either control (solid gray bars) or anti-Spike (hatched bars) serum for 1 h prior to addition to the cells. At 3 days postinfection, luciferase substrate reagent was added, and the luminescence was measured. The results are the means ± the SD of nine measurements from three independent experiments. When not visible, the SD values were contained within the size of the symbols. Anti-Spike serum either significantly decreased (VeroE6) or increased (THP-1, Raji, and Daudi) entry of SARS-CoVpp. ⁎, $P < 0.001$ (unpaired Student *t* test).

son's limiting dilution procedure, and expression of the transgene was confirmed by RT-PCR (data not shown) and flow cytometry (see Fig. 6A).

Lysosomotropic agent and protease inhibitor treatments. Cells were preincubated with the indicated amounts of drugs, either ammonium chloride (NH_4Cl) or E-64d/cathepsin L inhibitor (Cat L Inh; Calbiochem), for 1 h or 3 h prior to infection, respectively. SARS-CoVpp, pretreated with immune or control serum, were mixed with the same concentrations of drugs in tubes and added to the cells. After 5 h (E-64d or Cat L Inh) or 7 h (NH_4Cl), the cells were washed and further incubated with fresh medium without any drug. Cells were assayed for luciferase activity 60 to 65 h after infection, as described above.

Statistical analysis. Results are shown as means ± the standard deviations (SD) of the indicate number of observations. The statistical difference between groups was determined by using an unpaired Student *t* test with a 0.05 significance level.

RESULTS

Anti-Spike immune serum promotes the infection of human hematopoietic cells by SARS-CoV. SARS-CoV-induced pathology is not confined to the respiratory tract but also involves other tissues and organs, most importantly cells of the gastrointestinal tract and the immune system (19, 39, 74). Although several reports have shown that SARS-CoV can infect hematopoietic cells, it is not known how the virus gets a foothold into these immune cells that do not express the specific SARS-CoV receptor ACE2 (20, 21).

In order to investigate the possibility of antibody-mediated infection of immune cells during SARS pathogenesis, we have taken advantage of SARS-CoV Spike-pseudotyped particles (SARS-CoVpp) to compare the effect of anti-Spike immune serum on the prototypic permissive VeroE6 cells and a panel of immune cell lines (Fig. 1A). These recombinant viruses encoding a reporter gene and bearing the SARS-CoV Spike protein at the virion surface have been shown to faithfully mimic the SARS-CoV entry process (57, 71). As expected, SARS-CoVpp efficiently infected VeroE6 cells, whereas the luminescence signal detected in any of the immune cell types never exceeded values measured in the absence of SARS-CoVpp (Fig. 1B). To explore the occurrence of antibody-mediated infection, we preincubated SARS-CoVpp with either mouse anti-Spike immune-serum (Fig. 1A and B, hatched bars) or control serum (Fig. 1A and B, solid gray bars) prior to infection and then compared the resulting luminescence signal intensities.

The outcome of infection with SARS-CoVpp in the presence of anti-Spike immune-serum depended on the target cell type. Although heat-inactivated serum inhibited SARS-CoVpp entry into the permissive VeroE6 cell line in a dose-dependent fashion, as demonstrated by a dramatic drop in the intensity of luminescence (Fig. 1A and B, hatched bars), it facilitated infection of the human monocytic cell line THP-1 and of the B cell lines Daudi and Raji. In contrast, no infection of these cell lines was noticed when SARS-CoVpp were preincubated with control serum (Fig. 1A and B, solid bars), and similar background levels of luminescence were detected in the presence of immune serum only (data not shown). Of note, infection of the THP-1, Raji, and Daudi cell lines by recombinant viral particles pseudotyped with the glycoprotein of the vesicular stomatitis virus (VSVpp; Fig. 1C) or no viral envelope protein (Δenv.pp; Fig. 1D) was never affected by the presence of anti-SARS-CoV Spike immune serum. These experiments indicate that anti-Spike antibodies facilitate infection of SARS-CoVpp—but not VSVpp or Δenv.pp—into distinct immune cell types.

Altered tropism of replication-competent SARS-CoV toward human immune cells in the presence of anti-Spike immune serum. Because Raji cells displayed the greatest susceptibility to antibody-mediated infection of SARS-CoVpp (Fig. 1A and B), we used this B-cell-derived human cell line to investigate whether a change of tropism could also be observed during infection with replication-competent SARS-CoV.

As reported previously (30), infection of permissive VeroE6 cells remained unchanged in the presence of control serum, whereas anti-Spike immune serum fully abrogated it (Fig. 2A). In contrast, when Raji cells were infected in the presence of anti-Spike immune-serum, detection of intracellular viral proteins (*viz.*, membrane and nucleocapsid) was markedly different from those infected in the presence of control serum (Fig. 2B). Such enhanced infection was also demonstrated at the molecular level, since the viral gene detection by conventional RT-PCR (i.e., endpoint PCR; Fig. 3A) fully paralleled the real-time quantitative PCR measurements (Fig. 3B). Compared to inoculum containing control serum, there was significantly enhanced detection of subgenomic viral RNA (sgRNA) and nucleocapsid genes observed in Raji cells infected in the presence of anti-Spike immune serum (Fig. 3B, $P < 0.001$). Although we never detected SARS-CoV proteins in cells challenged in the presence of control serum, trace amounts of PCR products related to SARS-CoV ORF1b (data not shown), nucleocapsid genes and other viral genomic and subgenomic RNA were detectable (Fig. 3). These background levels were likely the result of nonspecific binding/uptake of SARS-CoV. Taken together, these experiments indicate that anti-Spike serum can trigger infection of immune cells by live SARS-CoV, similarly to that observed with the pseudotyped viral particles.

Antibody-mediated enhancement of SARS-CoV infection in Raji cells leads to abortive infection. To assess the capability of SARS-CoV to productively replicate into ADE-infected Raji cells, we monitored by PCR the cellular viral load, as well as the release of SARS-CoV progeny into cell culture supernatant. As previously seen at 15 hours postinfection (hpi) (Fig. 3A), all samples were determined to be positive by endpoint PCR for the detection of SARS-CoV genomic RNA. At most of the time points, low but noticeably higher amounts of SARS-CoV sgRNA were visible in cells infected in the presence of anti-Spike serum (not shown). Such results are in accordance with the quantitative measurements of either positive (i.e., genomic and mRNA) or negative (i.e., subgenomic replicative intermediates) RNA strands, demonstrating an increased viral load at 6 hpi, followed by a continuing decrease of both viral RNA species with time so that no more difference between groups was noted later on (Fig. 4A). Interestingly, despite the detection of SARS-CoV nucleic acid, neither SARS-CoV membrane (not shown) nor nucleocapsid protein (Fig. 4B) were detected in cells infected in the absence or presence of control serum. In contrast, a significant percentage of SARS-CoV nucleocapsid protein-positive cells was visualized when infected in the presence of anti-Spike serum, although there was no evidence of productive virus replication and spread to infect other cells (Fig. 4B).

To allow multiple antibody-mediated infection cycles, cells were cultured in the continuous presence of control or anti-

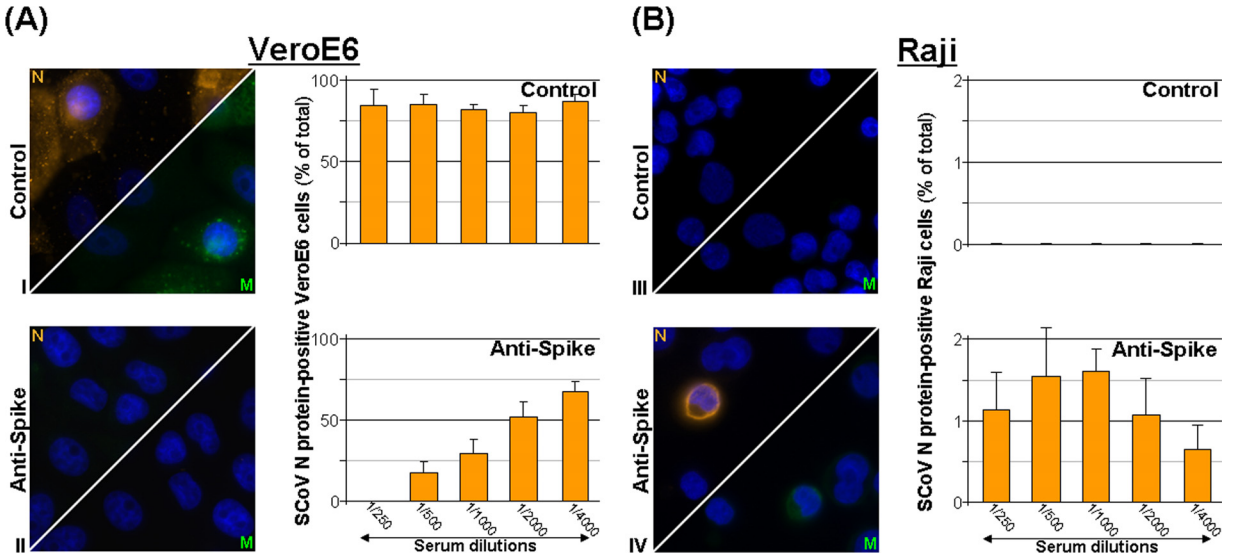

FIG. 2. Anti-Spike antibodies trigger SARS-CoV infection of human Raji B cells. VeroE6 or human Raji cells were infected (MOI = 1) with SARS-CoV strain HK39849 (SCoV) in the presence of either control or Anti-Spike serum for 1 h. Samples were fixed with 4% paraformaldehyde at 15 h postinfection. A mouse monoclonal antibody specific for the SCoV nucleocapsid (N) and rabbit polyclonal antibodies specific for SCoV membrane (M) protein were visualized using TRITC-conjugated goat anti-mouse and FITC-conjugated goat anti-rabbit antibodies, respectively. Cell nuclei were labeled with DAPI, and separate channel images were acquired. (A) As expected, SCoV infection of VeroE6 (I) was completely blocked by anti-Spike serum (1/500, II). (B) In contrast, SCoV viral proteins were detected in Raji cells only when they were incubated with anti-Spike (1/500, IV) but never with control serum (III). Quantification of infection (right-hand portions in panels A and B) was done by counting positive cells in 30 randomly chosen fields (630×, final magnification), using Metamorph as described in Materials and Methods. The results are shown as means ± the SD of the number of fields.

Spike serum. Because anti-Spike immune serum neutralized infection of permissive ACE2-bearing cells, it was not possible to titrate supernatants for infectious virus by 50% tissue culture infective dose ($TCID_{50}$) titration or plaque assays. Thus, real-time RT-PCR quantification of SARS-CoV viral genes in the culture supernatants was the only option available. As expected, we observed a concentration-dependent increase in the detection of both SARS-CoV ORF1b- and N-genes when supernatants of known $TCID_{50}$ titers were measured (Tables 1 and 2). Likewise, we detected increasing viral gene copies in cell culture supernatants of VeroE6 cells from > 1 to 7 to 9 days postinfection. Whereas the presence of control serum did not affect the virus titer, infection in the presence of anti-Spike immune serum significantly decreased it ($\log_{10}$ values of the nucleocapsid gene copies ± the SD at 9 days postinfection: SARS-CoV [6.22 ± 0.07] versus SARS-CoV + 1/1,000 control serum [5.88 ± 0.07] versus SARS-CoV + 1/1,000 anti-S serum [0.54 ± 0.13]). In contrast, we did not detect any change in viral gene copies when we assessed the viral load in supernatants of Raji-infected cells, whether incubated in the presence or absence of immune serum (Table 1).

Altogether, these results indicate that despite the ability of SARS-CoV to exploit antiviral antibodies to invade Raji B cells, only abortive replication occurs upon infection, and no infectious virus is released from the ADE-infected Raji cells.

The occurrence of ADE of SARS-CoV infection relies on the expression of human FcγRII (CD32) by the target cells. ADE involves several mechanisms, mostly through Fc receptor(s) (FcR) and complement receptor(s) (CR). Since ADE of SARS-CoV infection in our experimental setting occurred in the presence of heat-inactivated serum, we did not further investigate the contribution of CR to the observed phenomenon but, rather, focused on the possible participation of FcγR, which are expressed on the human leukocytes (9, 49).

Because we had previously shown the participation of FcγRII in antibody-mediated infection of Raji B cells (30), we examined by RT-PCR the expression profile of all the hematopoietic cell lines tested for susceptibility to antibody-mediated infection of SARS-CoVpp (Fig. 5A). The human immune cell lines displaying a detectable level of FcγR transcript were then subjected to flow cytometry (Fig. 5B). Our results indicate that U-937 and THP-1 exhibited cell surface expression of both FcγRI and FcγRIIA. As ascertained by RT-PCR, they express both the membrane-bound and the soluble isoforms of FcγRIIA (17, 66). The other cells express a single FcγR, except SUP-T1, MOLT-3, and ST486 (two T cell lines and a B cell line, respectively), which do not show detectable levels of any FcγR. Expression of FcγRIIA was detected in K-562 cell line, whereas the others predominantly display FcγRIIB. Of note, additional faint bands for the FcγRIIA were also seen in Raji cells (Fig. 5A and B).

Because THP-1, Raji, and Daudi cells are susceptible to ADE infection (Fig. 1) and because they express cell surface Fc receptor (Fig. 5), we investigated the effect of blocking individual FcγR on the occurrence of ADE infection (Fig. 5C). Although treatment with anti-FcγRI or anti-FcγRIII blocking antibody had virtually no effect on ADE in Raji and Daudi cells, blocking of FcγRII fully abrogated ADE infection of these cells. For THP-1, not only anti-FcγRII treatment decreased ADE infection, as expected, but also FcγRI (Fig. 5C). THP-1 cells indeed express both FcγRI and FcγRII, and intact antibodies could bind to the targeted FcγR via their Fab por-

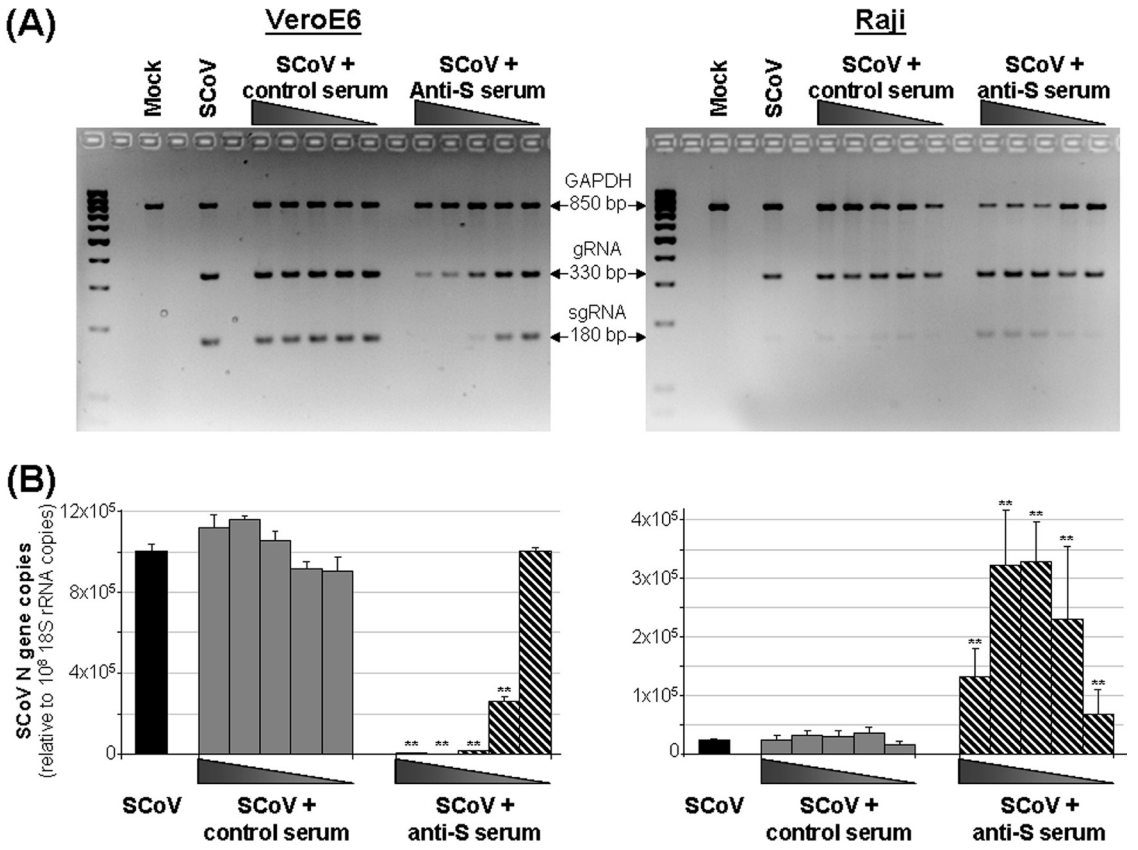

FIG. 3. Endpoint and real-time PCR detection of SARS-CoV genes in ADE-infected Raji cells. (A) VeroE6 and human Raji cells were incubated for 1 h in the absence (mock) or presence of SARS-CoV strain HK39849 (SCoV), with either control or anti-Spike (S) serum as indicated. The cells were lysed at 15 h postinfection, and total RNAs were extracted for RT-PCR amplification as described in Materials and Methods. Amplicons were visualized by ethidium bromide staining after agarose gel electrophoresis. A 1-kb molecular weight standard is shown on the left lane of each gel. (B) From the cDNA samples prepared in panel A, the levels of SCoV nucleocapsid and SCoV ORF1b (not shown) genes were determined by real-time quantitative RT-PCR. Raji cells were consistently infected in the presence of serial dilutions (1/250 to 1/4,000 in 2-fold dilutions) of anti-Spike serum that, in contrast, inhibited in dose-dependent fashion viral entry into the susceptible VeroE6 cells. The data are shown as the means ± the SD of four measurements from duplicate cultures and are representative of three independent experiments with similar results. **, $P < 0.001$ (unpaired Student t test).

tions and also to other FcγR expressed by the same cells via their Fc portion. Supporting this interpretation, anti-FcγRI is a mouse IgG1 that binds well to FcγRII, whereas anti-FcγRII is a mouse IgG2b that binds less efficiently to FcγRI (M. Daëron et al., unpublished observations).

To further establish the specific role of the FcγR subfamily in the ADE phenomenon, we stably transduced the ST486 B cell line, which is naturally deficient in the expression of the FcγR, with different constructs coding for FcγRIA (CD64a), FcγRIIA (CD32a), FcγRIIB1 (CD32b), and FcγRIIIA (CD16a). Moreover, due to allelic polymorphism of the human FcγRIIA and its alleged implications in disease susceptibility (48), we generated two variants of FcγRIIA bearing either a histidine (H) or an arginine (R) at amino acid position 131. As shown in Fig. 6, the parent ST486 cells were insensitive to both direct and antibody-mediated infection. Transduction of ST486 cells by lentiviral particles containing the different FcR coding sequences led to the generation of stable cell lines highly expressing the mRNA transgene (not shown), as well as the encoded FcγR at the plasma membrane (Fig. 6A). Similarly to the parental ST486 cells, FcγR-expressing cells were not permissive to direct SARS-CoVpp infection, regardless of their receptor subtype (Fig. 6B). However, when cells were infected in the presence of anti-SARS-CoV Spike immune-serum (Fig. 6B, hatched bars), ST486 expressing FcγRII became susceptible to antibody-mediated infection. Although both FcγRII members—FcγRIIA and FcγRIIB1—mediated enhanced SARS-CoVpp immune complex infectivity, we found that FcγRIIA appeared to do so more efficiently. Both FcγRIA and FcγRIIIA were unable to mediate ADE despite the wide range of serum dilutions that were tested (Fig. 6B).

Antibody-mediated infection by SARS-CoV does not rely on pH- and protease-dependent entry pathways. To compare the cellular requirements of ACE2- and FcR-mediated infection pathways, we investigated the effect of treatments with lysosomotropic agent and protease inhibitors on ADE. As previously described (24, 71), the addition of ammonium chloride (NH_4Cl), which prevents acidification of endosomal/lysosomal compartments, caused a dose-dependent reduction of SARS-CoVpp infection in ACE2-expressing VeroE6 cells (Fig. 7A, black squares). Similar treatment of Raji cells did not inhibit, but instead further enhanced antibody-mediated infection of

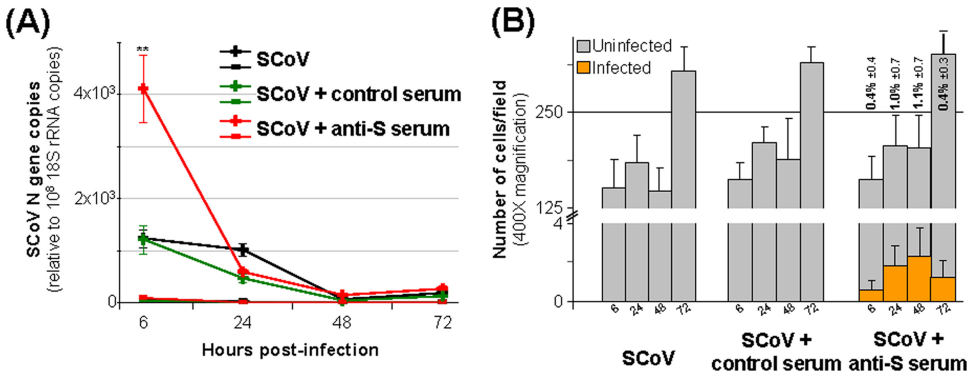

FIG. 4. Abortive replication of SARS-CoV in Raji cells following antibody-mediated infection. (A) Human Raji cells were incubated for 1 h in the absence or presence of SARS-CoV strain HK39849 (SCoV), with 2-fold serial dilutions (1/250 to 1/4,000) of either control or anti-Spike (S) serum. Cells were lysed at 6, 24, 48, and 72 hpi, and total RNAs were extracted and reverse transcribed into sense-specific cDNA species as described in Materials and Methods. The levels of positive (+) and negative (−) SCoV nucleocapsid strands were determined by real-time quantitative RT-PCR. For the sake of clarity, only one serum dilution (1/1,000) is shown. At an early time point (6 hpi), a high viral load was consistently detected in cells infected in the presence of anti-Spike but not in control serum. At later times (24 to 72 hpi), no further difference among the treatments was noticeable. The data are shown as means ± the SD of four measurements. When not visible, the SD values were contained within the size of the symbols. **, $P < 0.001$ (unpaired Student t test). (B) Human Raji cells infected as indicated in panel A were fixed with 4% paraformaldehyde, and costaining for SCoV nucleocapsid and cell nuclei was performed as described in Materials and Methods. Quantification of the infected and uninfected cells was done by counting 10 randomly chosen fields using Metamorph software. For the sake of clarity, results for only one serum dilution (1/1,000) are shown. Cell numbers and related percentage of infection are shown as means ± the SD of the number of observations. SCoV infection of Raji cells occurred only in the presence of anti-Spike serum, but the percentage of infected cells did not significantly increase over time.

SARS-CoVpp (Fig. 7A, red circles). Incubation of VeroE6 cells with both the broad cysteine protease inhibitor E-64d, as well as the more specific cathepsin L inhibitor III, abrogated ACE2-mediated infection (26, 56) (Fig. 7C and D, black squares), whereas E-64d did not have any impact on the ADE pathway, and only a partial reduction of ADE of SARS-CoVpp was observed in Raji with the highest tested concentrations of cathepsin L inhibitor III (Fig. 7C and D, red circles).

In these experiments, we noticed that neutralization of the endosome/lysosome acidification enhanced the infectivity of anti-Spike immune-serum-treated SARS-CoVpp (Fig. 7A, red circles). This observation raised the possibility that alkalinization of cells was associated with an increased expression of FcγR at the cell surface. Because Raji cells only express FcγRII (Fig. 5 and 6), we explored its expression levels at the cell surface after treatment with ammonium chloride. Our data indicate that surface expression of FcγRII was not increased (but, rather, slightly decreased) at 1, 3, and 5 h postinfection in the presence of NH_4Cl (Fig. 7B). Together, these results demonstrate that the two receptor-mediated infection processes, via ACE2 and FcγRII, follow very distinct cellular pathways.

Immune sera elicited by different SARS vaccine candidates mediate distinctly different profiles of virus neutralizing or enhancing activity. The SARS-CoV Spike glycoprotein, shown to be responsible for receptor binding to cellular ACE2, has been hypothesized to be a promising target for the development of both vaccines and therapeutics (14). Because we previously reported that anti-Spike sera can trigger SARS-CoV

TABLE 1. Viral yield in culture supernatants of SARS-CoV-infected Raji cells

Sample and treatment	Time (h) postinfection	Viral titer (log_{10} $TCID_{50}$/ml)	Mean no. (log_{10}) ± SD	
			ORF1b gene copies	Nucleocapsid gene copies
SARS-CoV inoculum (no treatment)		3	3.28 ± 0.04	3.41 ± 0.07
		5	5.39 ± 0.04	5.51 ± 0.08
		6	6.76 ± 0.05	6.94 ± 0.07
Cell culture supernatant from Raji cells				
No treatment	6 to 72	ND[a]	0	0
SARS-CoV + 1/1,000 control serum	6	ND	3.05 ± 0.15	3.56 ± 0.37
	24	ND	3.24 ± 0.13	3.84 ± 0.46
	48	ND	3.10 ± 0.03	3.50 ± 0.53
	72	ND	3.30 ± 0.04	3.65 ± 0.43
SARS-CoV + 1/1,000 anti-S serum	6	ND	3.36 ± 0.14	3.89 ± 0.41
	24	ND	2.84 ± 0.14	3.46 ± 0.50
	48	ND	3.26 ± 0.04	3.67 ± 0.50
	72	ND	3.43 ± 0.03	3.73 ± 0.38

[a] ND, not determined. The $TCID_{50}$ titration was not possible due to the presence of neutralizing immune serum in some cell culture supernatants. Results are shown as means ± the SD of four samples from two independent measurements.

TABLE 2. Primer sequences for RT-PCR detection of human transcripts of FcRs, ACE2, and GAPDH[a]

FcRs, ACE2, or GAPDH	Primer sequence (5′-3′)		Expected product size (bp)						
	Forward	Reverse	FcγR1A	FcγR2A	FcγR2B	FcγR3A	FcεR1γ-chain	ACE2	GAPDH
FcγR 1A	TgTCATgCgTggAAggATAA	TCgCACCAgTATAACCCAgAg	413						
FcγR 2A	TTgACAgTTTTgCTgCTgCT	AgCCTTCACAggATCAgTgg		702					
FcγR 2B	TTgCCACTgAgAgTgACTgg	ATTgTgTTCTCAgCCCCAAC			841				
FcγR 3A	CCTCCCAACTgCTCTg CTAC	ggTTgACACTgCCAAACCTT				580			
FcεR1γ-chain	ggAgAgCCTCAgCTCT gCTA	TggTggTTTCTCATgCTTCA					198		
ACE2	CAAgCAgCTgAggCCATTA	ATgCTAgggTCCAgggTTCT						1,190	
GAPDH	CAATgACCCCTTCATT gACC	TgCTgTAgCCAAATTCgTTG							866

[a] All sequences were designed using the Primer 3 Plus web-based application (64).

infection of immune cells, we have now compared the humoral immune responses elicited by five human SARS-CoV Spike-based immunogens.

The preparations consisted of either a whole killed SARS-CoV virion (WKV) or recombinant SARS-CoV Spike proteins (Fig. 8A) that had been immunopurified from cell lysates or cell culture supernatants. When compared by ELISA for binding activity against immobilized-recombinant SARS-CoV Spike full-length protein, all sera except for the control group displayed similar binding activity to recombinant Spike (Fig. 8D). Strong neutralizing humoral immune responses against SARS-CoVpp were detected in sera from animals immunized with recombinant Spike proteins or whole killed-SARS-CoV virion (Fig. 8B). Sera elicited by immunization with Ssol and WKV exhibited the highest neutralizing capabilities with 50% neutralizing titers of about 1/15,000 and 1/12,000, respectively, followed by sera immunized with S1 (1/8,000), S (1/4,000), and S.ECD (1/3,000). As expected, virtually no inhibition of SARS-CoVpp entry was observed in VeroE6 cells with control serum from mock-immunized BALB/c mice. When sera were tested for their ability to trigger ADE, they fell into two distinct groups (Fig. 8C). Although serum from WKV- and S.ECD-immunized mice had no effect, Ssol, S1, and S immune sera triggered the infection of Raji cells. We reasoned that these differences might have been the consequence of the specific immune response triggered by the distinct immunogens and immunization protocols and, therefore, we determined the relative amount of anti-Spike IgG subclasses of the immune sera (Fig. 8D). Of note, we observed that the ADE-inducing sera did not contain anti-Spike IgG2a antibodies, which were present in all neutralizing/nonenhancing sera. These results suggest that the relative amounts of IgG subclass may be involved in determining the occurrence of antibody-mediated infection of SARS-CoV.

DISCUSSION

The possibility that an immune response to pathogens may have also deleterious effects on the host homeostasis has been the focus of several studies. For example, the hyperinduction of cytokines following avian influenza virus infection has been implicated in the severity of the disease (47), and infection of cells by antibody-dependent enhancement has been known to occur for several viral diseases (59, 60). We demonstrate here that anti-Spike antibody potentiates infection of immune cells by SARS Spike-pseudotyped lentiviral particles and replication-competent SARS-coronavirus. Antibody-mediated infection is dependent on one subtype of Fcγ receptor, FcγRII (CD32). However, ADE mediated by FcγRII does not utilize the endosomal/lysosomal pathway utilized by ACE2-bound virus, i.e., the common cellular receptor for SARS-CoV in susceptible cells. Finally, we have found evidence that this ADE phenomenon is dependent on the immunization strategy used for candidate vaccines.

We and others (14, 15, 51) reasoned that SARS-CoV Spike glycoprotein, which has been shown to be responsible for viral attachment and entry, was a prime target for the development of SARS vaccines. Because of earlier reports of immune-mediated enhancement of coronavirus infection both *in vitro* (8, 44, 73) and *in vivo* (65, 68), we investigated this possibility and reported preliminary data that a neutralizing, anti-Spike immune-serum induced ADE of SARS-CoVpp (30). The effect of SARS-CoV antiviral antibodies on ADE has been studied in susceptible cells, but conflicting data have appeared. One group demonstrated antibody-dependent enhancement of lentiviral particles pseudotyped with SARS-CoV Spike variants detected in palm civets when incubated with rodent (vaccine-elicited) and convalescent SARS patient-derived monoclonal antibodies (73). In contrast, another group, using panels of isogenic SARS-CoV, did not find any evidence of infection enhancing potential with a series of monoclonal antibodies (50).

Our experiments conclusively demonstrate with several lines of evidence that both SARS-CoVpp and replication-competent SARS-coronavirus infect certain immune cells only in the presence of anti-Spike immune serum and not in its absence. Furthermore, we found that homologous anti-Spike immune-serum never potentiated infection of the permissive epithelial cell line VeroE6.

In cells infected via the ADE pathway we detected both SARS-CoV genomic and subgenomic material, as well as the expression of two viral proteins, N and M. It is believed that an antibody-mediated infection pathway could provide SARS-CoV additional entry routes, allowing the virus to broaden its tropism. Interestingly, early after ADE infection, we detected far more (ca. 50- to 100-fold) SARS-CoV-positive RNAs compared to its negative strand, a situation found during the productive replication of coronaviruses (55) and distinct from the abortive replication of SARS-CoV reported after direct infection of macrophages (7). Although we unambiguously illus-

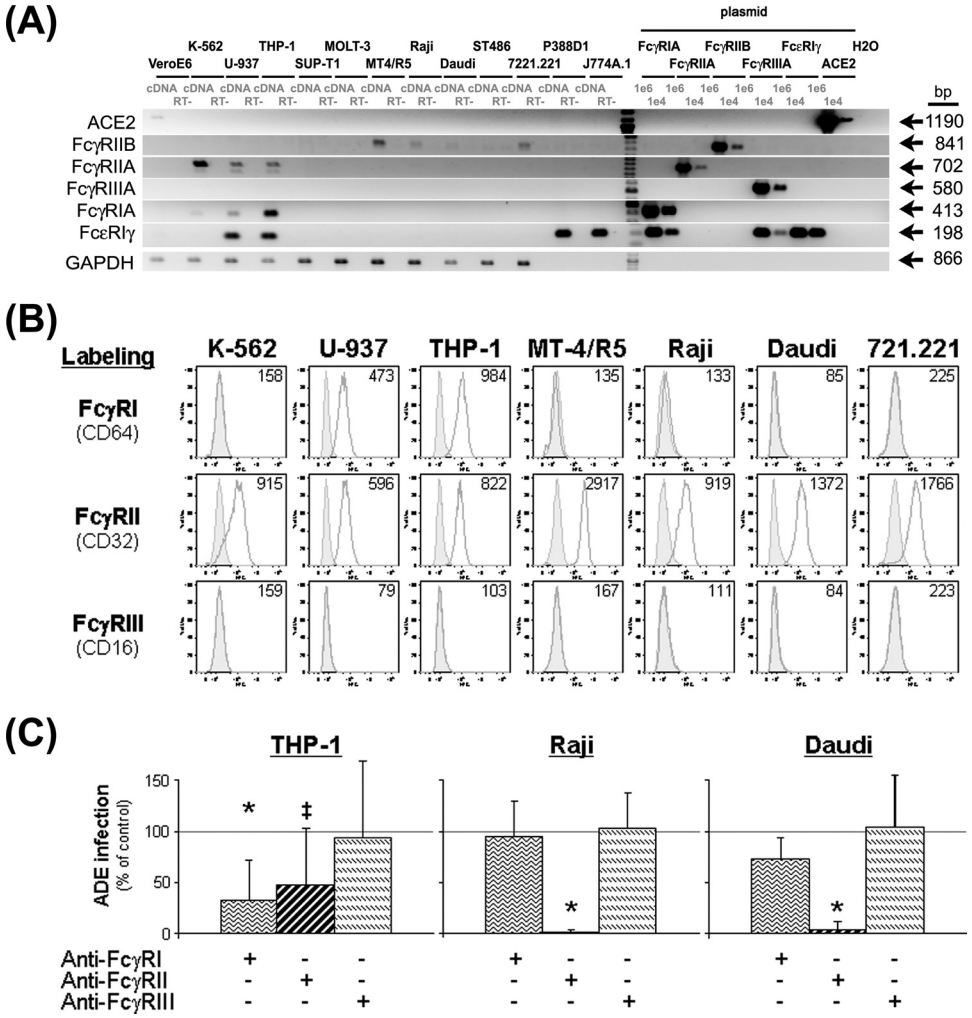

FIG. 5. Blockade of FcγRII abrogates antibody-mediated infection of human immune cell lines. (A) Total RNAs from the indicated cell lines were extracted for RT-PCR amplification as described under Materials and Methods. cDNAs and negative RT controls (RT−) were probed for detection of FcεR1γ-chain, FcγRIA (CD64a), FcγRIIA (CD32a), FcγRIIB (CD32b), FcγRIIIA (CD16a), ACE2, and GAPDH. DNA plasmids containing the coding sequence of the human Fc receptors or the human ACE2 (10^4 and 10^6 copies) were used as positive controls. Amplicons were visualized by ethidium bromide staining after agarose gel electrophoresis. For reference, a 1-kb molecular-weight standard is also shown. Due to the murine origin of the macrophage-like P388D1 and J774A.1 cell lines and because the primers were designed for the detection of human FcR (Table 2), no FcγR transcripts were detected in P388D1 and J774A.1 cells. (B) Hematopoietic cell lines displaying a detectable level of FcγR transcript in panel A were subjected to flow cytometry. Cell lines were stained with either isotype-matched control antibody (gray-filled histograms) or FcγR-specific mouse monoclonal antibody (open histograms) as indicated, followed by secondary FITC-conjugated goat anti-mouse antibodies. Labeled samples were then read by flow cytometry and post-acquisition analysis was performed using FlowJo software. Insets show the median of fluorescence intensity of the anti-FcγR staining. When not visible, the open histograms were superimposed on the gray-filled ones. The data are representative of two independent experiments with similar results. (C) Effect of FcγR blockage on susceptibility of the cells to ADE infection. Prior to infection, cells were treated with anti-FcγR blocking antibodies. At 3 days postinfection, luciferase substrate reagent was added to wells, and the luminescence was measured. The data were normalized to control conditions, *viz.*, cells infected in the presence of IgG isotype-matched control antibody, and expressed as a percentage of the changes in luminescence. For all conditions, values of background luminescence (never exceeding 3% of control) were subtracted prior to normalization. The results are the means ± the SD of nine measurements from three independent experiments. ‡, $P < 0.05$; *, $P < 0.001$ (unpaired Student *t* test).

trated ongoing infection thanks to the detection of *de novo* synthesis of the structural viral proteins N and M, the ADE-infected Raji cells did not support productive replication of SARS-CoV. After the initiation of viral gene transcription and viral protein synthesis, a block appears to occur in the replication process, ultimately ending in an abortive viral cycle without the detectable release of progeny virus (12). Whether ADE occurs in other immune cells and whether such infection will be abortive remains to be investigated.

Despite not leading to productive infection, it remains of interest to investigate the functionality and cell fate of ADE infected cells. Thus, ADE infection induced the initiation of viral gene transcription—with production of viral gene intermediate species—and viral protein synthesis. Given the ability of intracellular innate immune sensors, such as the pattern recognition receptor families TLR and RLH, to detect viral gene species (2, 69) and the disturbance to the cell homeostasis caused by SARS-CoV viral proteins (such as 3a protein and

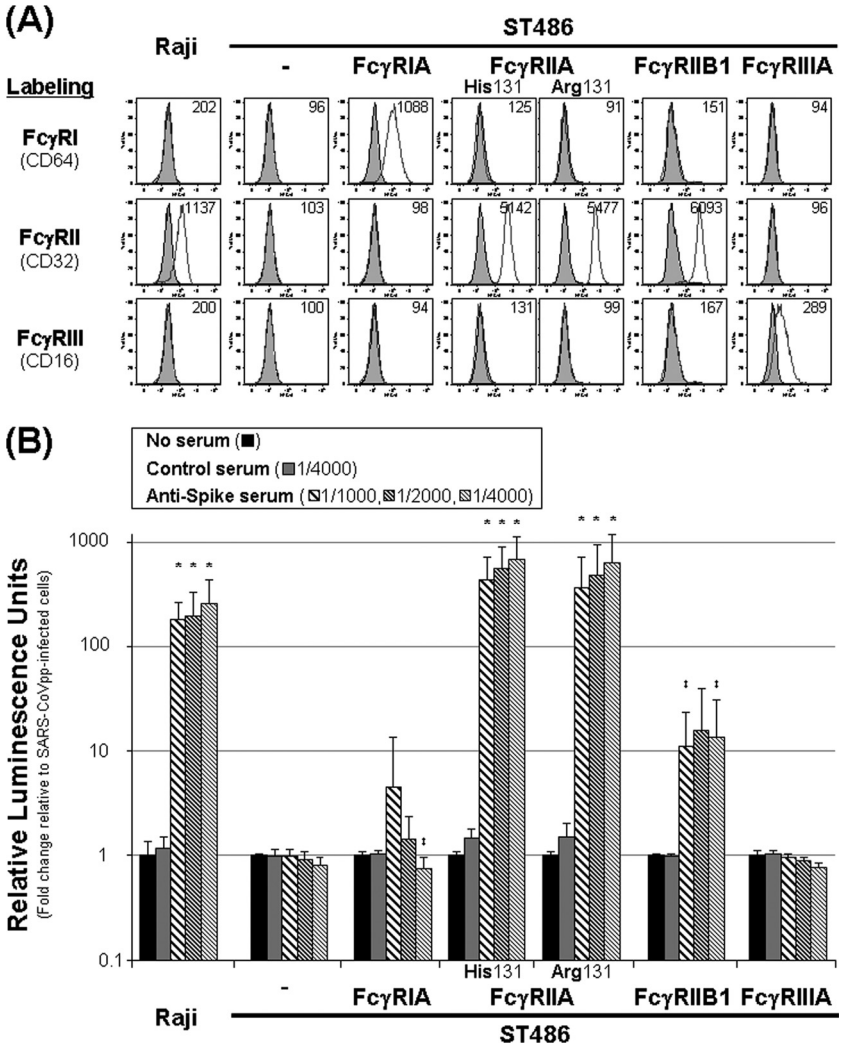

FIG. 6. Human FcγRIIA and B1, but not huFcγRIA nor huFcγRIIIA, are responsible for ADE of SARS-CoV pseudoparticles (SARS-CoVpp) infection. (A) Human Raji, parental, and monoclonal FcγR-transduced human ST486 B cell lines were stained with either isotype-matched control antibody (gray-tinted histogram) or FcγR-specific mouse monoclonal antibody (open histogram) as indicated, followed by secondary FITC-conjugated goat anti-mouse antibodies. Labeled samples were then read by flow cytometry and postacquisition analysis was performed using FlowJo software. The inset shows the median of fluorescence intensity of the anti-FcγR staining. When not visible, the open histograms were superimposed on the gray-filled ones. (B) Potency of FcγR(s) to trigger antibody-mediated entry of SARS-CoVpp was assessed by using ST486 cell lines stably expressing a single FcγR. SARS-CoVpp were incubated in the presence or absence of different dilutions (1/1,000, 1/2,000, and 1/4,000) of either control (solid bars) or anti-Spike (hatched bars) serum for 1 h prior to addition to the cells. At 3 days postinfection, luciferase substrate reagent was added to wells, and the luminescence was measured. The data were normalized to control conditions, *viz.*, cells incubated with SARS-CoVpp in the absence of any serum (black bar, taken as unity) and expressed as fold changes in luminescence. Because results for SARS-CoVpp ± control serum were virtually identical with all cell lines, for the sake of clarity only one dilution (1/4,000) is shown. The results are the means ± the SD of nine measurements from three independent experiments. Statistical significance was assessed by comparing the appropriate dilutions of mock and anti-Spike serum. ‡, $P < 0.05$; ∗, $P < 0.01$ (unpaired Student *t* test).

SARS-unique domain) (5, 36, 63), a possible participation of immune-mediated enhanced disease during SARS pathogenesis cannot be ruled out. Of note, clinical observations have already reported poor disease outcomes in early seroconverted SARS patients (22, 37, 76).

The observation of a change of tropism of SARS-CoV in the presence of antiviral immune serum distinguishes the ADE of SARS-CoV infection from many other examples of antibody-mediated viral infection, where the presence of antiviral antibodies increases the viral load due to infection of a higher number of already-susceptible cells (59, 60). Of note, a shift of tropism from epithelial to immune cells, albeit mediated by a different mechanism, was associated with an increased severity of disease during the course of lethal coronavirus-induced feline infectious peritonitis (52).

FcγR blocking experiments clearly demonstrate the involvement of FcγRII in the occurrence of ADE infection of Raji and Daudi cells. Since both anti-FcγRI and anti-FcγRII treatments, however, had an impact on the occurrence of ADE infection of THP-1 cells, no firm conclusion could be drawn as for the possible contribution of FcγRI. Due to the coexpression of the two FcγR in this cell line (cf. Fig. 5B, where ~100%

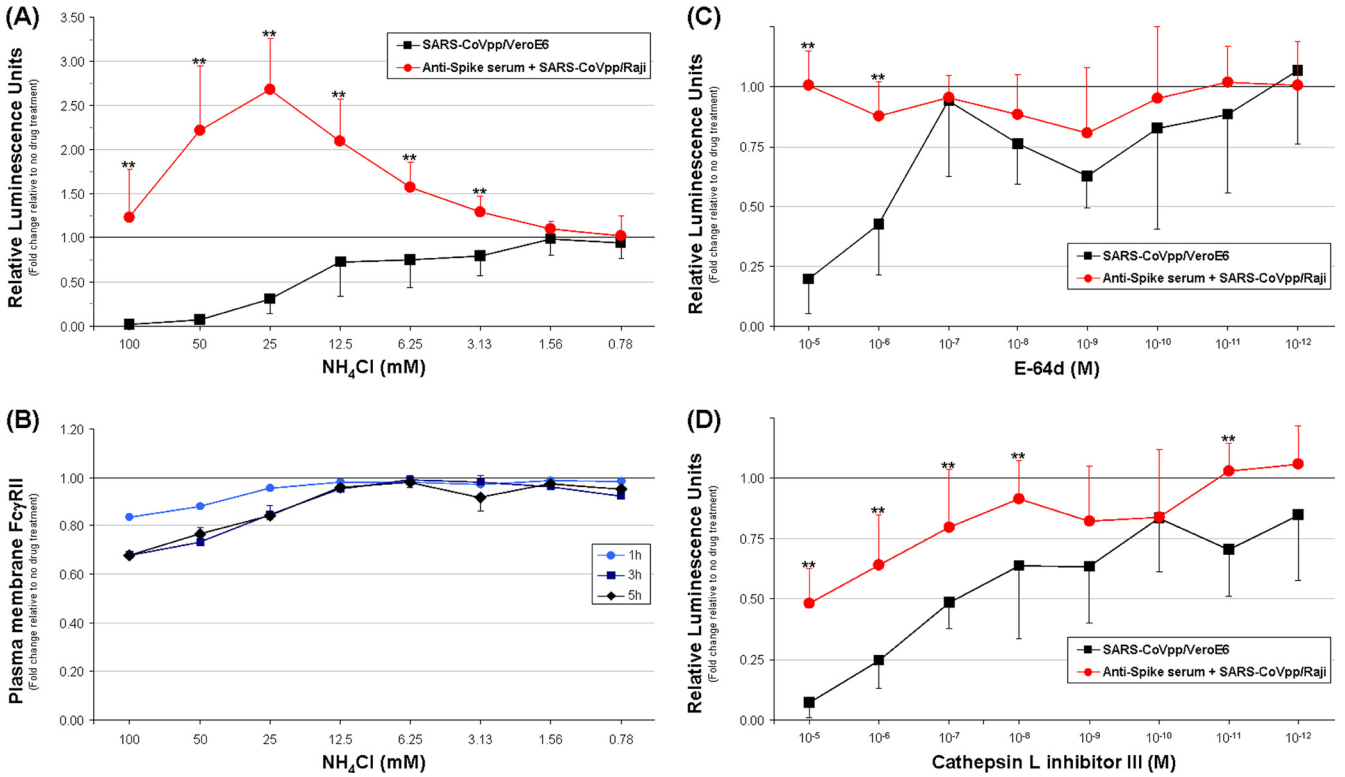

FIG. 7. Antibody-mediated infection is independent of acidic pH and cysteine-protease activity of the endosomal/lysosomal compartment. (A, C, and D) pH and protease requirements for ACE2- versus antibody-mediated entry of SARS-CoVpp were investigated with different pharmacological treatments. Prior to infection, VeroE6 and Raji cells were preincubated with the indicated concentrations of ammonium chloride (NH_4Cl) (A) for 1 h or the cysteine protease inhibitor E-64d (C) and cathepsin L inhibitor III (D) for 3 h. SARS-CoVpp, with or without anti-Spike serum (1/2,000), were then added to the cells in the continuous presence of the drugs. At 3 days postinfection, luciferase substrate reagent was added to wells, and the luminescence was measured. The data were normalized to the appropriate control conditions (taken as unity) with SARS-CoVpp with or without anti-Spike serum for Raji and VeroE6 cells, respectively. The results are shown as means ± the SD of nine measurements from three independent experiments. Statistical differences between VeroE6 and Raji cells were assessed by the unpaired Student *t* test. **, $P < 0.005$. (B) Cell surface expression of FcγRII on Raji cells after NH_4Cl treatment. Cells were incubated with the indicated concentrations of the drug for 1, 3, and 5 h, labeled with anti-huFcγRII antibody, and subjected to flow cytometry. The data were normalized to the mean fluorescence intensity of controls (no drug). The results are shown as means ± the SD of six measurements from two independent experiments. When not visible, the SD values were contained within the size of the symbols.

of the cells expressed FcγRI and FcγRII), blocking antibodies could indeed bind not only to the targeted FcγR via their Fab portions but also to other FcγR via their Fc portions. Thus, for example, mouse IgG1 anti-FcγRI antibody could bind specifically to FcγRI via its Fab portions and to FcγRII via its Fc portion, making both FcγR unavailable for interacting with opsonized pseudoparticles.

On the basis of these results, we decided to undertake a systematic analysis of the individual role of the human Fcγ receptors subfamilies. Our experiments demonstrate that only FcγRIIA and, to a lesser extent, FcγRIIB1 triggered infection by SARS-CoVpp in the presence of anti-Spike serum. These results extend our observations with FcγR-blocking antibodies in Raji cells (30) because only FcγRII, but not FcγRI or FcγRIII, is found in that cell line. However, in light of the IgG composition of the anti-Spike immune serum used in the present study and of the inability of FcγRI and FcγRIII to bind mouse IgG1 (10), further investigations are required to formally rule out the involvement of these receptors in triggering ADE of SARS.

Despite these results suggesting an important role of the FcγRII family in the occurrence of ADE of SARS-CoV, our conclusion has to be qualified by the observation that other human immune cell lines (such as K-562, U-937, MT4-R5, and 721.221) that also have detectable cell surface expression of FcγRII by flow cytometry are refractory to ADE infection. The ability of those cell lines to bind SARS-CoVpp/anti-Spike immune complexes is now under investigation. If binding and/or internalization occurs, it would also be of interest to ensure that failure of infection is not due to inability of the viral particles to uncoat/initiate replication in those cells. Finally, in order to define more precisely the mechanism underlying the susceptibility of immune cells to antibody-mediated SARS-CoV infection, a better understanding of the events downstream binding of the immune complexes to the Fc receptors is needed.

Viral glycoproteins typically mediate attachment, fusion, and entry by one of two mechanisms. Some viruses, such as HIV, infect mainly through a pH-independent entry process (fusion occurring at the plasma membrane), whereas other viruses, such as influenza, utilize a pH-dependent endocytic pathway (31). It has been demonstrated that, following binding

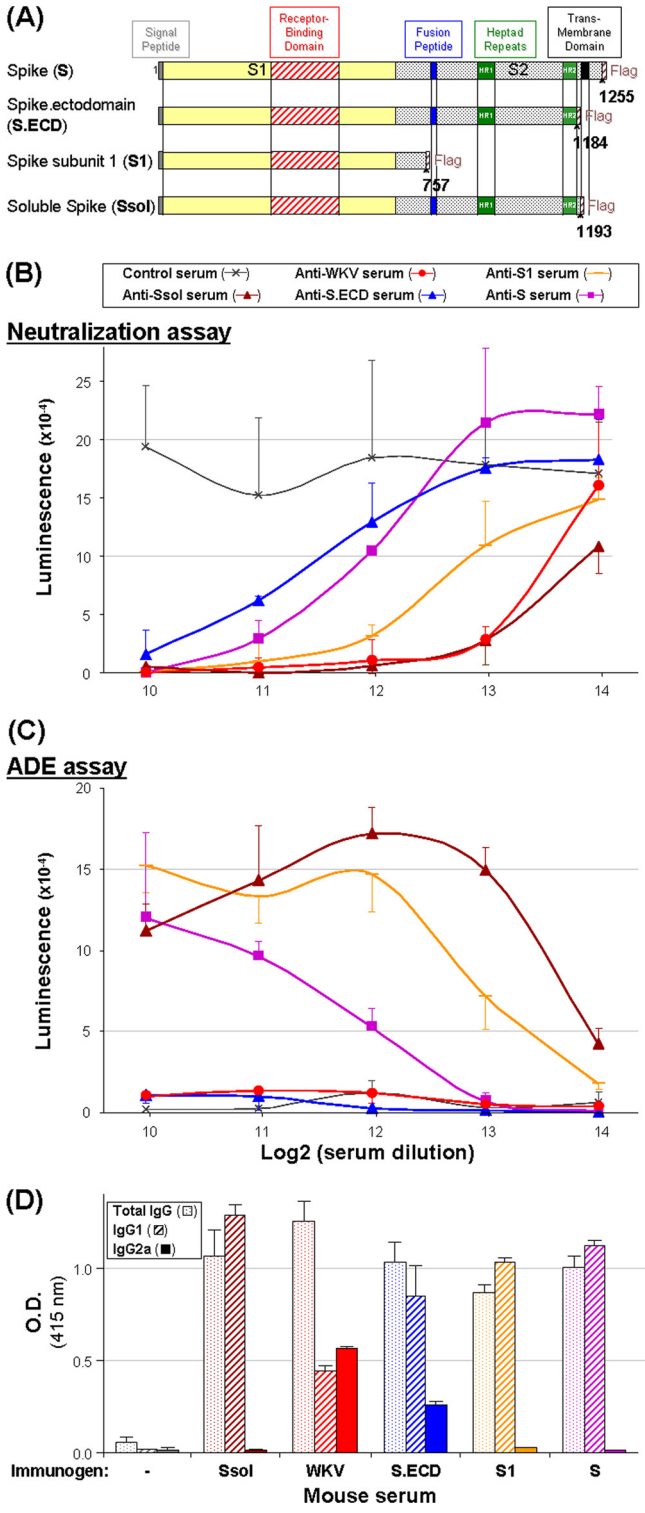

FIG. 8. Occurrence of ADE of SARS-CoV infection after immunization with different vaccine candidates. (A) Schematic illustration of the different forms of recombinant SARS-CoV Spike protein used for vaccination of BALB/c mice. Positions of the different regions are indicated according to Swiss-Prot accession no. P59594. (B and C) Neutralizing and enhancing abilities of antisera elicited after immunization with different SARS vaccine candidates. SARS-CoVpp were incubated in the presence of a 2-fold serial dilution (1/1,000 to 1/16,000) of either control or anti-Spike serum for 1 h prior to addition to VeroE6 cells (B) (neutralization assay) or Raji cells (C) (ADE assay). At 3 days postinfection, luciferase substrate reagent was added to the wells, and the luminescence was measured. Five independent experiments were performed in triplicates, and data are presented as the means ± the SD of a representative experiment. (D) IgG composition of the immune serum of mice vaccinated with the indicated immunogens. The binding activity toward immobilized recombinant SARS-CoV Spike protein of pooled serum (1/2,000 dilution) was measured by ELISA, and bound IgGs were revealed with specific polyclonal secondary antibodies. A representative result from three independent experiments is shown. The results are expressed as means ± the SD of triplicate measurements. When not visible, the SD values were contained within the size of the symbols.

to its ACE2 receptor, SARS-CoV entry into susceptible cells occurs via pH-dependent endocytosis (24, 71), although Spike protein can also induce cell fusion at a neutral pH (40, 57). More recently a crucial activity of the lysosomal cysteine protease cathepsin L for an efficient infection by SARS-CoV has been uncovered (26, 56). In contrast, our results indicate that Fc receptor-mediated infection is not dependent on either endosomal acidic pH or the activity of cysteine proteases.

A striking observation was the opposite outcome of the ACE2- versus FcγR-mediated infection subsequent to neutralization of the endosomal acidic pH. Whereas infection of VeroE6 cells was completely inhibited by NH_4Cl, as previously described (24, 71), the same treatment triggered an approximately 2- to 4-fold increase in ADE infection. The exacerbation of the antibody-mediated infection in the presence of NH_4Cl is not due to a higher cell surface expression of the FcγRII, which was actually slightly decreased. A likely explanation for our results would be that most of the viral particles that enter cells through ADE pathway remain trapped in an acidic compartment and are eventually degraded. The inhibition of endosomal acidification prevents their degradation and grants them opportunity to accumulate and more efficiently infect cells upon removal of the drug at 7 h postinfection. Alternatively, the ability of Spike to mediate cell membrane fusion at neutral pH (40, 57), could allow more antibody-opsonized SARS-CoVpp to fuse with the endosomal membranes. Such a mechanism has already been observed with a poorly infectious HIV strain, which exhibited greatly enhanced infectivity under conditions where endosomal pH was neutralized (16, 67). Taken together, our results demonstrate that the biochemical requirements of FcγR-mediated infection are markedly distinct from those underlying ACE2-dependent entry and illustrate a novel mechanism by which SARS-CoV can enter into target cells.

The emergence of SARS in late 2002, which resulted in significant human and economic losses, highlighted the lack of antiviral strategies to control coronavirus infections. Given the continuous presence of SARS-CoV related agents in the environmental reservoir, vaccination remains a major option for preventing resurgence of SARS in humans, especially individuals at highest risk in the case of an outbreak (i.e., healthcare workers). Some vaccines against animal coronaviruses have been successfully generated, but their development has proven very difficult due to immune enhancement of disease in vaccinated recipients (28, 53, 65).

We have evaluated, therefore, the neutralizing versus en-

hancing capabilities of 5 different SARS vaccine formulations. Our results show that ADE was dependent on the immunization strategy with two of five candidate vaccines displaying obvious neutralizing capabilities without triggering SARS-CoVpp entry into immune cells. It is not clear why the other three formulations induced ADE while showing similar neutralizing potencies. We can rule out the lack of recognition/binding to SARS-CoVpp, since all tested sera displayed a clear dose-dependent neutralization of the viral particles over at least four serial dilutions. Furthermore, the total IgG content was comparable among the immunized cohorts, except for the control group that, as expected, had a lower amount (data not shown).

In the FCoV model, ADE has been linked to both neutralizing and non-neutralizing antibodies (8). In our experiments we have observed that, among sera causing ADE there was a direct correlation between the neutralization titer and the enhancing capability. Because anti-SARS-CoV Spike sera were able to both neutralize SARS-CoVpp infection and bind native recombinant full-length Spike protein with similar potency (i.e., Ssol $\approx$ WKV $\gg$ S1 $>$ S $\geq$ S.ECD), we speculate that vaccination with a given immunogen did not induce a marked bias in eliciting non-neutralizing anti-Spike IgGs. However, we cannot exclude that variations in the ratio of neutralizing versus non-neutralizing epitopes between vaccine preparations could have an impact on the occurrence of ADE.

Because a single class of anti-FCoV Spike antibodies (i.e., IgG2a) has been demonstrated to play a crucial role in initiation of ADE (8, 25), we have investigated the relative amount of anti-Spike IgG1 and IgG2a in our mouse sera. Interestingly, none of the ADE-inducing sera contained anti-Spike IgG2a antibodies, whereas the two neutralizing/nonenhancing sera did. Further experiments are needed to understand why a markedly distinct polarization of the immune response was achieved with highly related SARS-CoV Spike immunogens and whether absence of IgG2a is causally related to the occurrence of ADE infection.

Recently, allelic polymorphism of the human FcγRIIA has been incriminated as a risk factor for developing severe SARS pathology (75). The authors of that study found that individuals harboring the R/R131 genotype were more likely to develop severe SARS pathology than were their H/H131 counterparts. The R/R131 form of FcγRIIA can bind to both IgG1 and IgG2a, whereas H/H131 can only bind to IgG2a (48, 54). However, in our transduction experiments using B cell clones stably expressing a single polymorphic FcγRIIA, both allelic variants were able to trigger ADE of SARS-CoVpp.

It is usually agreed that infection by SARS-CoV is not only confined to the respiratory tract but also involves the gastrointestinal tract and other organ systems. Several reports have highlighted the direct infection of hematopoietic cells by SARS-CoV (19, 39, 74); however, it is not yet clear how SARS-CoV gets a foothold into immune cells, which do not express the SARS-CoV receptor ACE2 (20, 21). Antibody-mediated infection, in addition to other alternative entry routes, such as L-SIGN or DC-SIGN (29, 71), may provide SARS-CoV with an opportunity to broaden its target options. Interestingly, antibody-mediated infection has been shown to elicit markedly distinct responses compared to viral entry through the natural host receptor (23, 45, 58, 62). Indeed, antibody-mediated infection of feline coronavirus not only enhances viral progeny but also dramatically increases production of tumor necrosis factor alpha by infected cells. The hyperinduction of the proinflammatory cytokine is believed to account for the exacerbated apoptosis of the neighboring leukocytes (61, 62). Similarly, ADE of Ross river virus has been shown to facilitate viral replication by disrupting transcription of antiviral type I interferons (58). Because it has been hypothesized that deregulation of host cytokine/chemokine responses is a hallmark of SARS (7, 27, 35, 43, 70), it would be interesting to investigate how ADE of SARS-CoV infection may contribute to the disease pathogenesis.

Altogether, our results report a novel mechanism by which SARS-CoV can enter into target cells that do not express the conventional virus receptor and are otherwise refractory to the virus. This may have implications for understanding the tropism and pathogenesis of the virus and highlight potential pitfalls associated with immunization against this coronavirus. These findings should prompt further investigations for a better understanding of the molecular and cellular mechanisms underlying ADE of SARS-CoV infection. The consequences of this alternative infection pathway on the functionality and/or homeostasis of the target cells also need to be resolved.

ACKNOWLEDGMENTS

We thank Rik Gijsbers and Zeger Debyser (Katholieke Universiteit Leuven, Leuven, Belgium) for providing the bicistronic retroviral vector used to establish the FcγR-expressing stable cell lines. We also thank Clark L. Anderson (Ohio State University, Columbus, OH), Jacob J. Schlesinger (University of Rochester Medical Center, Rochester, NY), Jean-Pierre Kinet (Harvard Medical School, Boston, MA), and Lewis L. Lanier (University of California, San Francisco, CA) for generously providing original cDNAs for human FcγRIA (CD64a), FcεRγ-chain, and FcγRIIIA (CD16a), respectively. We also thank Kwok Hung Chan (Queen Mary Hospital, Pokfulam, Hong Kong, People's Republic of China) for the gift of the mouse monoclonal antibody (4D11) specific for the SARS-CoV nucleoprotein and Valérie Lorin (Institut Pasteur, Paris, France) for expert technical assistance. Finally, we thank the members of the HKU-Pasteur Research Centre for expert advice and helpful discussion.

This study was supported by the Research Fund for the Control of Infectious Disease (projects 05050182 and 09080872) of the Hong Kong Government, by the RESPARI project of the Institut Pasteur International Network, and in part by grants from GlaxoSmithKline Biologicals. B.C. was supported by a fellowship from GlaxoSmithKline Biologicals.

REFERENCES

1. **Bisht, H., et al.** 2004. Severe acute respiratory syndrome coronavirus spike protein expressed by attenuated vaccinia virus protectively immunizes mice. Proc. Natl. Acad. Sci. U. S. A. **101:**6641–6646.
2. **Brennan, K., and A. G. Bowie.** 2010. Activation of host pattern recognition receptors by viruses. Curr. Opin. Microbiol. **13:**503–507.
3. **Buchholz, U. J., et al.** 2004. Contributions of the structural proteins of severe acute respiratory syndrome coronavirus to protective immunity. Proc. Natl. Acad. Sci. U. S. A. **101:**9804–9809.
4. **Callendret, B., et al.** 2007. Heterologous viral RNA export elements improve expression of severe acute respiratory syndrome (SARS) coronavirus spike protein and protective efficacy of DNA vaccines against SARS. Virology **363:**288–302.
5. **Chan, C. M., et al.** 2009. The ion channel activity of the SARS-coronavirus 3a protein is linked to its pro-apoptotic function. Int. J. Biochem. Cell Biol. **41:**2232–2239.
6. **Chen, J., and K. Subbarao.** 2007. The Immunobiology of SARS*. Annu. Rev. Immunol. **25:**443–472.

7. **Cheung, C. Y., et al.** 2005. Cytokine responses in severe acute respiratory syndrome coronavirus-infected macrophages in vitro: possible relevance to pathogenesis. J. Virol. **79:**7819–7826.
8. **Corapi, W. V., C. W. Olsen, and F. W. Scott.** 1992. Monoclonal antibody analysis of neutralization and antibody-dependent enhancement of feline infectious peritonitis virus. J. Virol. **66:**6695–6705.
9. **Daëron, M.** 1997. Fc receptor biology. Annu. Rev. Immunol. **15:**203–234.
10. **Daëron, M.** 1999. Fc receptors, p. 43–121. *In* M. Zanetti and J. D. Capra (ed.), The antibodies, vol. 5. Harwood Academic Publishers, Amsterdam, Netherlands.
11. **Daniel, C., and P. J. Talbot.** 1990. Protection from lethal coronavirus infection by affinity-purified spike glycoprotein of murine hepatitis virus, strain A59. Virology **174:**87–94.
12. **David, A., et al.** 2006. The engagement of activating FcγRs inhibits primate lentivirus replication in human macrophages. J. Immunol. **177:**6291–6300.
13. **Drosten, C., et al.** 2003. Identification of a novel coronavirus in patients with severe acute respiratory syndrome. N. Engl. J. Med. **348:**1967–1976.
14. **Du, L., et al.** 2009. The spike protein of SARS-CoV: a target for vaccine and therapeutic development. Nat. Rev. Microbiol. **7:**226–236.
15. **Enjuanes, L., et al.** 2008. Vaccines to prevent severe acute respiratory syndrome coronavirus-induced disease. Virus Res. **133:**45–62.
16. **Fredericksen, B. L., B. L. Wei, J. Yao, T. Luo, and J. V. Garcia.** 2002. Inhibition of endosomal/lysosomal degradation increases the infectivity of human immunodeficiency virus. J. Virol. **76:**11440–11446.
17. **Fridman, W. H., et al.** 1993. Soluble Fcγ receptors. J. Leukoc. Biol. **54:**504–512.
18. **Gillim-Ross, L., et al.** 2004. Discovery of novel human and animal cells infected by the severe acute respiratory syndrome coronavirus by replication-specific multiplex reverse transcription-PCR. J. Clin. Microbiol. **42:**3196–3206.
19. **Gu, J., et al.** 2005. Multiple organ infection and the pathogenesis of SARS. J. Exp. Med. **202:**415–424.
20. **Hamming, I., et al.** 2004. Tissue distribution of ACE2 protein, the functional receptor for SARS coronavirus: a first step in understanding SARS pathogenesis. J. Pathol. **203:**631–637.
21. **Harmer, D., M. Gilbert, R. Borman, and K. L. Clark.** 2002. Quantitative mRNA expression profiling of ACE 2, a novel homologue of angiotensin converting enzyme. FEBS Lett. **532:**107–110.
22. **Ho, M. S., et al.** 2005. Neutralizing antibody response and SARS severity. Emerg. Infect. Dis. **11:**1730–1737.
23. **Hober, D., W. Chehadeh, A. Bouzidi, and P. Wattre.** 2001. Antibody-dependent enhancement of coxsackievirus B4 infectivity of human peripheral blood mononuclear cells results in increased interferon-alpha synthesis. J. Infect. Dis. **184:**1098–1108.
24. **Hofmann, H., et al.** 2004. S protein of severe acute respiratory syndrome-associated coronavirus mediates entry into hepatoma cell lines and is targeted by neutralizing antibodies in infected patients. J. Virol. **78:**6134–6142.
25. **Hohdatsu, T., et al.** 1998. Antibody-dependent enhancement of feline infectious peritonitis virus infection in feline alveolar macrophages and human monocyte cell line U937 by serum of cats experimentally or naturally infected with feline coronavirus. J. Vet. Med. Sci. **60:**49–55.
26. **Huang, I. C., et al.** 2006. SARS coronavirus, but not human coronavirus NL63, utilizes cathepsin L to infect ACE2-expressing cells. J. Biol. Chem. **281:**3198–3203.
27. **Huang, K. J., et al.** 2005. An interferon-gamma-related cytokine storm in SARS patients. J. Med. Virol. **75:**185–194.
28. **Huisman, W., B. E. Martina, G. F. Rimmelzwaan, R. A. Gruters, and A. D. Osterhaus.** 2009. Vaccine-induced enhancement of viral infections. Vaccine **27:**505–512.
29. **Jeffers, S. A., et al.** 2004. CD209L (L-SIGN) is a receptor for severe acute respiratory syndrome coronavirus. Proc. Natl. Acad. Sci. U. S. A. **101:**15748–15753.
30. **Kam, Y. W., et al.** 2007. Antibodies against trimeric S glycoprotein protect hamsters against SARS-CoV challenge despite their capacity to mediate FcγRII-dependent entry into B cells in vitro. Vaccine **25:**729–740.
31. **Kielian, M., and F. A. Rey.** 2006. Virus membrane-fusion proteins: more than one way to make a hairpin. Nat. Rev. Microbiol. **4:**67–76.
32. **Kuiken, T., et al.** 2003. Newly discovered coronavirus as the primary cause of severe acute respiratory syndrome. Lancet **362:**263–270.
33. **Lanier, L. L., G. Yu, and J. H. Phillips.** 1989. Co-association of CD3ζ with a receptor (CD16) for IgG Fc on human natural killer cells. Nature **342:**803–805.
34. **Lau, S. K., et al.** 2005. Severe acute respiratory syndrome coronavirus-like virus in Chinese horseshoe bats. Proc. Natl. Acad. Sci. U. S. A. **102:**14040–14045.
35. **Law, H. K., et al.** 2005. Chemokine up-regulation in SARS-coronavirus-infected, monocyte-derived human dendritic cells. Blood **106:**2366–2374.
36. **Law, P. T., et al.** 2005. The 3a protein of severe acute respiratory syndrome-associated coronavirus induces apoptosis in Vero E6 cells. J. Gen. Virol. **86:**1921–1930.
37. **Lee, N., et al.** 2006. Anti-SARS-CoV IgG response in relation to disease severity of severe acute respiratory syndrome. J. Clin. Virol. **35:**179–184.
38. **Letourneur, O., et al.** 1991. Characterization of the family of dimers associated with Fc receptors (Fc epsilon RI and Fc gamma RIII). J. Immunol. **147:**2652–2656.
39. **Li, L., et al.** 2003. SARS-coronavirus replicates in mononuclear cells of peripheral blood (PBMC) from SARS patients. J. Clin. Virol. **28:**239–244.
40. **Li, W., et al.** 2003. Angiotensin-converting enzyme 2 is a functional receptor for the SARS coronavirus. Nature **426:**450–454.
41. **Miller, K. L., A. M. Duchemin, and C. L. Anderson.** 1996. A novel role for the Fc receptor gamma subunit: enhancement of Fc gamma R ligand affinity. J. Exp. Med. **183:**2227–2233.
42. **Nefkens, I., et al.** 2007. Hemagglutinin pseudotyped lentiviral particles: characterization of a new method for avian H5N1 influenza serodiagnosis. J. Clin. Virol. **39:**27–33.
43. **Nicholls, J. M., et al.** 2003. Lung pathology of fatal severe acute respiratory syndrome. Lancet **361:**1773–1778.
44. **Olsen, C. W., W. V. Corapi, C. K. Ngichabe, J. D. Baines, and F. W. Scott.** 1992. Monoclonal antibodies to the spike protein of feline infectious peritonitis virus mediate antibody-dependent enhancement of infection of feline macrophages. J. Virol. **66:**956–965.
45. **Palmer, P., B. Charley, B. Rombaut, M. Daëron, and P. Lebon.** 2000. Antibody-dependent induction of type I interferons by poliovirus in human mononuclear blood cells requires the type II Fcγ receptor (CD32). Virology **278:**86–94.
46. **Park, S., et al.** 1998. Immune response of sows vaccinated with attenuated transmissible gastroenteritis virus (TGEV) and recombinant TGEV spike protein vaccines and protection of their suckling pigs against virulent TGEV challenge exposure. Am. J. Vet. Res. **59:**1002–1008.
47. **Peiris, J. S., C. Y. Cheung, C. Y. Leung, and J. M. Nicholls.** 2009. Innate immune responses to influenza A H5N1: friend or foe? Trends Immunol. **30:**574–584.
48. **Rascu, A., R. Repp, N. A. Westerdaal, J. R. Kalden, and J. G. van de Winkel.** 1997. Clinical relevance of Fc gamma receptor polymorphisms. Ann. N. Y. Acad. Sci. **815:**282–295.
49. **Ravetch, J. V., and S. Bolland.** 2001. IgG Fc receptors. Annu. Rev. Immunol. **19:**275–290.
50. **Rockx, B., et al.** 2008. Structural basis for potent cross-neutralizing human monoclonal antibody protection against lethal human and zoonotic severe acute respiratory syndrome coronavirus challenge. J. Virol. **82:**3220–3235.
51. **Roper, R. L., and K. E. Rehm.** 2009. SARS vaccines: where are we? Expert Rev. Vaccines **8:**887–898.
52. **Rottier, P. J., K. Nakamura, P. Schellen, H. Volders, and B. J. Haijema.** 2005. Acquisition of macrophage tropism during the pathogenesis of feline infectious peritonitis is determined by mutations in the feline coronavirus spike protein. J. Virol. **79:**14122–14130.
53. **Saif, L. J.** 2004. Animal coronavirus vaccines: lessons for SARS. Dev. Biol. (Basel) **119:**129–140.
54. **Salmon, J. E., et al.** 1996. Fc gamma RIIA alleles are heritable risk factors for lupus nephritis in African Americans. J. Clin. Invest. **97:**1348–1354.
55. **Sawicki, S. G., and D. L. Sawicki.** 1986. Coronavirus minus-strand RNA synthesis and effect of cycloheximide on coronavirus RNA synthesis. J. Virol. **57:**328–334.
56. **Simmons, G., et al.** 2005. Inhibitors of cathepsin L prevent severe acute respiratory syndrome coronavirus entry. Proc. Natl. Acad. Sci. U. S. A. **102:**11876–11881.
57. **Simmons, G., et al.** 2004. Characterization of severe acute respiratory syndrome-associated coronavirus (SARS-CoV) spike glycoprotein-mediated viral entry. Proc. Natl. Acad. Sci. U. S. A. **101:**4240–4245.
58. **Suhrbier, A., and M. La Linn.** 2003. Suppression of antiviral responses by antibody-dependent enhancement of macrophage infection. Trends Immunol. **24:**165–168.
59. **Sullivan, N. J.** 2001. Antibody-mediated enhancement of viral disease. Curr. Top. Microbiol. Immunol. **260:**145–169.
60. **Takada, A., and Y. Kawaoka.** 2003. Antibody-dependent enhancement of viral infection: molecular mechanisms and in vivo implications. Rev. Med. Virol. **13:**387–398.
61. **Takano, T., et al.** 2007. A "possible" involvement of TNF-alpha in apoptosis induction in peripheral blood lymphocytes of cats with feline infectious peritonitis. Vet. Microbiol. **119:**121–131.
62. **Takano, T., T. Hohdatsu, A. Toda, M. Tanabe, and H. Koyama.** 2007. TNF-alpha, produced by feline infectious peritonitis virus (FIPV)-infected macrophages, upregulates expression of type II FIPV receptor feline aminopeptidase N in feline macrophages. Virology **364:**64–72.
63. **Tan, J., et al.** 2009. The SARS-unique domain (SUD) of SARS coronavirus contains two macrodomains that bind G-quadruplexes. PLoS Pathog. **5:**e1000428.
64. **Untergasser, A., et al.** 2007. Primer3Plus, an enhanced web interface to Primer3. Nucleic Acids Res. **35:**W71–W74.
65. **Vennema, H., et al.** 1990. Early death after feline infectious peritonitis virus challenge due to recombinant vaccinia virus immunization. J. Virol. **64:**1407–1409.
66. **Warmerdam, P. A., J. G. van de Winkel, E. J. Gosselin, and P. J. Capel.** 1990.

Molecular basis for a polymorphism of human Fc gamma receptor II (CD32). J. Exp. Med. **172:**19–25.
67. **Wei, B. L., et al.** 2005. Inhibition of lysosome and proteasome function enhances human immunodeficiency virus type 1 infection. J. Virol. **79:**5705–5712.
68. **Weingartl, H., et al.** 2004. Immunization with modified vaccinia virus Ankara-based recombinant vaccine against severe acute respiratory syndrome is associated with enhanced hepatitis in ferrets. J. Virol. **78:**12672–12676.
69. **Wilkins, C., and M. Gale, Jr.** 2010. Recognition of viruses by cytoplasmic sensors. Curr. Opin. Immunol. **22:**41–47.
70. **Wong, C. K., et al.** 2004. Plasma inflammatory cytokines and chemokines in severe acute respiratory syndrome. Clin. Exp. Immunol. **136:**95–103.
71. **Yang, Z. Y., et al.** 2004. pH-dependent entry of severe acute respiratory syndrome coronavirus is mediated by the spike glycoprotein and enhanced by dendritic cell transfer through DC-SIGN. J. Virol. **78:**5642–5650.
72. **Yang, Z. Y., et al.** 2004. A DNA vaccine induces SARS coronavirus neutralization and protective immunity in mice. Nature **428:**561–564.
73. **Yang, Z. Y., et al.** 2005. Evasion of antibody neutralization in emerging severe acute respiratory syndrome coronaviruses. Proc. Natl. Acad. Sci. U. S. A. **102:**797–801.
74. **Yilla, M., et al.** 2005. SARS-coronavirus replication in human peripheral monocytes/macrophages. Virus Res. **107:**93–101.
75. **Yuan, F. F., et al.** 2005. Influence of FcγRIIA and MBL polymorphisms on severe acute respiratory syndrome. Tissue Antigens **66:**291–296.
76. **Zhang, L., et al.** 2006. Antibody responses against SARS coronavirus are correlated with disease outcome of infected individuals. J. Med. Virol. **78:**1–8.